![USGS science for a changing world]

Potential Effects of Groundwater Pumping on Water Levels, Phreatophytes, and Spring Discharges in Spring and Snake Valleys, White Pine County, Nevada, and Adjacent Areas in Nevada and Utah

Scientific Investigations Report 2011–5032

U.S. Department of the Interior
U.S. Geological Survey

Potential Effects of Groundwater Pumping on Water Levels, Phreatophytes, and Spring Discharges in Spring and Snake Valleys, White Pine County, Nevada, and Adjacent Areas in Nevada and Utah

By Keith J. Halford and Russell W. Plume

U.S. Department of the Interior
KEN SALAZAR, Secretary

U.S. Geological Survey
Marcia K. McNutt, Director

U.S. Geological Survey, Reston, Virginia: 2011

Contents

Figures

Figures—Continued

Tables

Conversion Factors and Datums

Multiply	By	To obtain
Length		
inch (in.)	2.54	centimeter (cm)
foot (ft)	0.3048	meter (m)
mile (mi)	1.609	kilometer (km)
Area		
acre	4,047	square meter (m^2)
acre	0.004047	square kilometer (km^2)
square foot (ft^2)	0.09290	square meter (m^2)
square mile (mi^2)	2.590	square kilometer (km^2)
Volume		
acre-foot (acre-ft	1,233	cubic meter (m^3)
Flow rate		
acre-foot/yr (acre-ft/yr)	1,233	cubic meter per year (m^3/yr)
foot per year (ft/yr)	0.3048	meter per year (m/yr)
cubic foot per second (ft^3/s)	0.02832	cubic meter per second (m^3/s)
cubic foot per day (ft^3/d)	0.02832	cubic meter per day (m^3/d)
gallons per minute (gal/min)	0.06309	liter per second (L/s)
Hydraulic conductivity		
foot per day (ft/d)	0.3048	meter per day (m/d)
Transmissivity		
foot squared per day (ft^2/d)	0.09290	meter squared per day (m^2/d)
Leakance		
foot per day per foot [(ft/d)/ft]	1	meter per day per meter

Temperature in degrees Celsius (°C) may be converted to degrees Fahrenheit (°F) as follows:

$$°F=(1.8×°C)+32.$$

Temperature in degrees Fahrenheit (°F) may be converted to degrees Celsius (°C) as follows:

$$°C=(°F-32)/1.8.$$

Transmissivity: The standard unit for transmissivity is cubic foot per day per square foot times foot of aquifer thickness [(ft^3/d)/ft^2]ft. In this report, the mathematically reduced form, foot squared per day (ft^2/d), is used for convenience.

Specific conductance is given in microsiemens per centimeter at 25 degrees Celsius (μS/cm at 25°C).

Concentrations of chemical constituents in water are given either in milligrams per liter (mg/L) or micrograms per liter (μg/L).

Datums

Vertical coordinate information is referenced to the North American Vertical Datum of 1988 (NAVD 88).

Horizontal coordinate information is referenced to the North American Datum of 1983 (NAD 83).

Altitude, as used in this report, refers to distance above the vertical datum.

Potential Effects of Groundwater Pumping on Water Levels, Phreatophytes, and Spring Discharge in Spring and Snake Valleys, White Pine County, Nevada, and Adjacent Areas in Nevada and Utah

By Keith J. Halford and Russell W. Plume

Abstract

Assessing hydrologic effects of developing groundwater supplies in Snake Valley required numerical, groundwater-flow models to estimate the timing and magnitude of capture from streams, springs, wetlands, and phreatophytes. Estimating general water-table decline also required groundwater simulation. The hydraulic conductivity of basin fill and transmissivity of basement-rock distributions in Spring and Snake Valleys were refined by calibrating a steady state, three-dimensional, MODFLOW model of the carbonate-rock province to predevelopment conditions. Hydraulic properties and boundary conditions were defined primarily from the Regional Aquifer-System Analysis (RASA) model except in Spring and Snake Valleys. This locally refined model was referred to as the Great Basin National Park calibration (GBNP-C) model. Groundwater discharges from phreatophyte areas and springs in Spring and Snake Valleys were simulated as specified discharges in the GBNP-C model. These discharges equaled mapped rates and measured discharges, respectively.

Recharge, hydraulic conductivity, and transmissivity were distributed throughout Spring and Snake Valleys with pilot points and interpolated to model cells with kriging in geologically similar areas. Transmissivity of the basement rocks was estimated because thickness is correlated poorly with transmissivity. Transmissivity estimates were constrained by aquifer-test results in basin-fill and carbonate-rock aquifers.

Recharge, hydraulic conductivity, and transmissivity distributions of the GBNP-C model were estimated by minimizing a weighted composite, sum-of-squares objective function that included measurement and Tikhonov regularization observations. Tikhonov regularization observations were equations that defined preferred relations between the pilot points. Measured water levels, water levels that were simulated with RASA, depth-to-water beneath distributed groundwater and spring discharges, land-surface altitudes, spring discharge at Fish Springs, and changes in discharge on selected creek reaches were measurement observations.

The effects of uncertain distributed groundwater-discharge estimates in Spring and Snake Valleys on transmissivity estimates were bounded with alternative models. Annual distributed groundwater discharges from Spring and Snake Valleys in the alternative models totaled 151,000 and 227,000 acre-feet, respectively and represented 20 percent differences from the 187,000 acre-feet per year that discharges from the GBNP-C model. Transmissivity estimates in the basin fill between Baker and Big Springs changed less than 50 percent between the two alternative models.

Potential effects of pumping from Snake Valley were estimated with the Great Basin National Park predictive (GBNP-P) model, which is a transient groundwater-flow model. The hydraulic conductivity of basin fill and transmissivity of basement rock were the GBNP-C model distributions. Specific yields were defined from aquifer tests. Captures of distributed groundwater and spring discharges were simulated in the GBNP-P model using a combination of well and drain packages in MODFLOW. Simulated groundwater captures could not exceed measured groundwater-discharge rates.

Four groundwater-development scenarios were investigated where total annual withdrawals ranged from 10,000 to 50,000 acre-feet during a 200-year pumping period. Four additional scenarios also were simulated that added the effects of existing pumping in Snake Valley. Potential groundwater pumping locations were limited to nine proposed points of diversion. Results are presented as maps of groundwater capture and drawdown, time series of drawdowns and discharges from selected wells, and time series of discharge reductions from selected springs and control volumes.

Simulated drawdown propagation was attenuated where groundwater discharge could be captured. General patterns of groundwater capture and water-table declines were similar for all scenarios. Simulated drawdowns greater than 1 ft propagated outside of Spring and Snake Valleys after 200 years of pumping in all scenarios.

Introduction

Currently, southern Nevada relies on the Colorado River for most of its water supply. Supplementary water supplies are needed to offset a persistent drought in the Colorado River Basin. Groundwater resources from basin-fill and consolidated-rock aquifers in eastern Nevada are a potential source for this supplemental water supply. These aquifers provide water to springs, streams, wetlands, limestone caves, and other biologically sensitive areas on Federal lands in eastern Nevada, which provide habitat for numerous species of plants and animals, including one species of federally listed endangered fish. These water-dependent features also are visited and enjoyed by anglers, hunters, and tourists, including numerous visitors to Great Basin National Park.

Assessing hydrologic effects of developing groundwater supplies in the Western United States can be greatly improved through use of groundwater models. Hydrologic effects typically include the timing and magnitude of capture from streams, springs, wetlands, and phreatophytes—deep rooted plants that obtain their water from the water table or the layer of deposits just above it. Assessments of general water-table decline initially were limited to simple analytic models of water-table decline—drawdown with a Theis (1935) solution and capture of groundwater discharge with a Glover and Balmer (1954) solution. These analytical solutions approximated hydrologic changes that were caused by new pumping wells.

Solving directly for change is a good method because the hydrologic effects of groundwater development typically are defined by drawdown and capture of groundwater discharge. Analytical solutions, however, cannot easily simulate complex aquifer geometry, heterogeneous hydraulic properties, or a wide range of surface-water features. Modern numerical models, however, allow for the inclusion of many additional hydrologic features and can be quite complex (Leake and others, 2008). Additional model complexity also has made model results more uncertain, which needlessly encourages more controversy in a historically contentious process. The relative simplicity of analytical solutions can be applied correctly by solving directly for change with numerical models.

Purpose and Scope

The purpose of this report is to estimate potential effects of water-supply development on water levels, phreatophytes, and spring discharges around the southern Snake Range in Spring and Snake Valleys. The effects of water-supply development were investigated with revised models of the carbonate-rock province as defined in the Great Basin Regional Aquifer-System Analysis (Prudic and others, 1995). Recharge, hydraulic conductivity, thickness of basin fill, and transmissivity were refined exclusively in Spring and Snake Valleys by calibrating a three-dimensional,

groundwater-flow model. Geometries of the hydrogeologic units within the area of interest (fig. 1) were refined and principally reflected findings from Elliott and others (2006). Transmissivity and specific-yield estimates were constrained from specific capacity, aquifer-test results, and analysis of multiple-year water-level declines in response to groundwater pumping. Groundwater-discharge areas in Spring and Snake Valleys were defined with results from the Basin and Range Carbonate-Rock Aquifer System (BARCAS) study (Welch and others, 2007). Potential effects of water-supply development on water levels and spring discharges were simulated with a variant of the calibrated model. This predictive model simulated ground-water discharge with the direct-drawdown approach where groundwater discharge is limited to observed locations and estimated rates.

Approach

Potential effects of groundwater development were assessed with the direct-drawdown approach in this study. Application of the direct-drawdown approach requires a groundwater-flow model for calibration and a separate model for prediction. Transmissivity distributions are estimated with the calibration model that simulates all relevant processes, including recharge. The predictive model uses the transmissivity distribution that was estimated with the calibration model and observed groundwater discharges. This approach is superior to modifying the calibration model because simulated and observed groundwater discharge will differ in the calibration model.

Direct simulation of drawdown can reduce model complexity and uncertainty because fewer hydrologic features need to be simulated in the predictive model. Model input, other than the proposed pumpage, is limited to hydraulic-conductivity, storage-coefficient, and groundwater-discharge distributions. Drawdown models simulate changes so relatively unchanging quantities, such as recharge and existing pumpage distributions, are not simulated and do not need to be defined. The absence of these features simplifies presentation of model results and avoids the large uncertainty associated with recharge and historical pumping estimates.

The U.S. Department of the Interior, National Park Service needed estimates of the potential effects of groundwater pumping from Snake Valley on springs, streams, and water levels in caves in and adjacent to Great Basin National Park (fig. 1). Understanding potential effects of groundwater pumping from Snake Valley is important because groundwater discharge to springs and streams in ecologically sensitive areas may be captured. This study estimates potential hydrologic effects of water-supply development in Spring and Snake Valleys by integrating hydrologic data from recent investigations (Elliott and others, 2006; Welch and others, 2007) in a broader regional framework (Prudic and others, 1995).
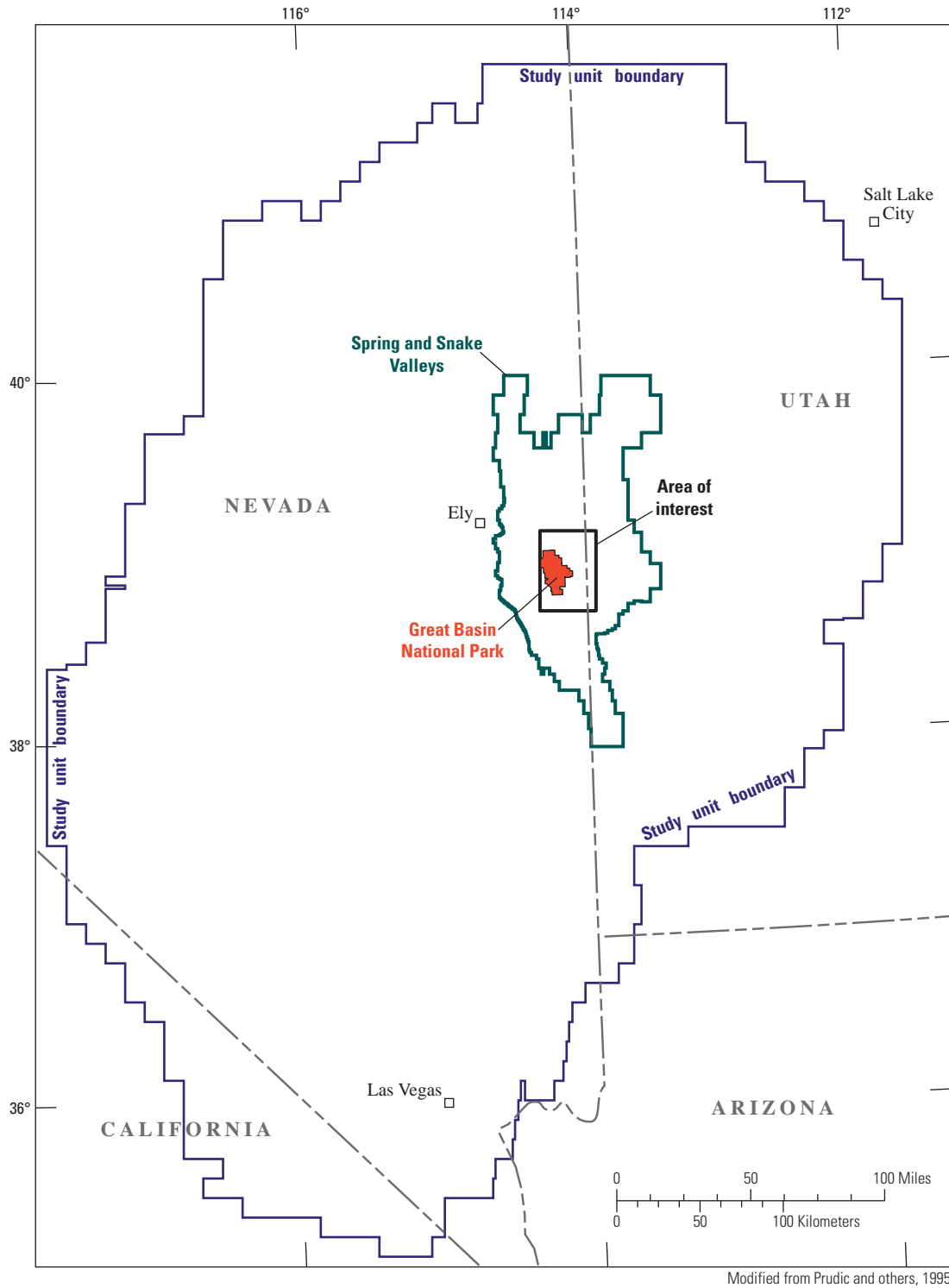
Figure 1. Location of study area, Spring and Snake Valleys, area of interest, and Great Basin National Park, Nevada.

Description of Study Area

The study area for this report is the 100,000 mi[2] carbonate-rock province of the Great Basin (fig. 1) as defined by Harrill and Prudic (1998). The study area was selected because groundwater flow was simulated previously for the Regional Aquifer-System Analysis (RASA) Program of the Great Basin (Prudic and others, 1995), and because pumping effects can propagate across multiple basins in the carbonate-rock province (Schaefer and Harrill, 1995). Aquifers in the study area comprise permeable basin-fill deposits or carbonate rocks (Harrill and Prudic, 1998).

Most of this investigation centers on Spring and Snake Valleys and the area of interest (fig. 1). The area of interest is southern Spring and Snake Valleys including the Great Basin National Park. Hydrogeologic interpretation was refined throughout Spring and Snake Valleys because these are defined hydrographic areas that encompass the area of interest.

Precipitation is the source of all water, both surface discharge and groundwater, in Spring and Snake Valleys. Groundwater recharge originates as high-altitude precipitation, and a small percentage of this becomes recharge primarily as infiltration of spring-snowmelt runoff along mountain fronts. Annual precipitation in mountainous areas generally exceeds 16 in. and has been estimated to exceed 40 in. on some of the high mountain ranges (PRISM Group, 2006). However, the area over which this precipitation falls constitutes only a small part of Spring and Snake Valleys. As a result, the total volume of precipitation available as potential groundwater recharge is relatively small. Total annual precipitation in basin lowlands generally ranges from 6 to 10 in. (Western Regional Climate Center, 2009). The area over which this range of precipitation falls constitutes a large part of Spring and Snake Valleys. However, very little of this precipitation becomes groundwater recharge because the precipitation is mostly lost as evaporation or is transpired by plants.

The topography of Spring and Snake Valleys is typical of the Great Basin section of the Basin and Range physiographic province. Basins and adjacent mountains generally are oriented north-south. Land-surface altitude in basin lowlands ranges from 4,300 ft in northern Snake Valley to 6,500 ft in southern Snake (Hamlin) Valley. Land-surface altitude in mountainous areas exceeds 13,000 ft in the southern Snake Range.

Hydrogeology

Spring and Snake Valleys are deep structural basins composed of carbonate and siliciclastic-sedimentary rocks of Paleozoic age and igneous intrusive rocks of Jurassic to Tertiary age. Basin-fill deposits of Tertiary and Quaternary age and volcanic rocks of Tertiary age have accumulated in these structural basins, reaching thicknesses of 5,000–10,000 ft (Sweetkind and others, 2007, pl. 1). For purposes of the present study, these rocks and deposits are divided into six hydrogeologic units that are from oldest to youngest: (1) low–permeability, siliciclastic-sedimentary rocks of early Cambrian and older age, and granitic rocks of Jurassic and Tertiary age; (2) permeable carbonate rocks of middle Cambrian to Devonian age and Mississippian to Permian age, and intervening siliciclastic-sedimentary rocks of Mississippian age; (3) low-permeability volcanic rocks of Tertiary age; (4) older sedimentary rocks of Miocene age; (5) low-permeability, fine-grained basin-fill deposits of Tertiary and Quaternary age; and (6) permeable coarse-grained basin-fill deposits of Quaternary age. The distribution and occurrence of each of the units is shown in figure 2 and their lithologic and hydrologic characteristics are summarized in figure 3.

The siliciclastic-sedimentary rocks of Cambrian and older age, and the granitic rocks of Jurassic to Tertiary age are grouped together as a single hydrogeologic unit because both have low permeability. The former consists mostly of metamorphosed quartzite and shale and the latter consist of granite, granodiorite, and quartz monzonite (Hose and others, 1976, p. 3–6 and 22–25). Quartzites can be highly fractured and potentially have significant secondary permeability. However, shales can be squeezed into fractures partly sealing off any secondary permeability (Winograd and Thordarson, 1975, p. 39–40). A general indication of its low permeability is that perennial mountain streams are restricted mostly to watersheds underlain by this hydrogeologic unit. This unit mostly impedes the movement of groundwater.

The carbonate and siliciclastic-sedimentary rocks of Cambrian to Permian age comprise three sequences: (1) carbonate rocks and minor interbedded siliciclastic-sedimentary rocks (shale and sandstone) of Cambrian to Devonian age; (2) siliciclastic-sedimentary rocks and minor carbonate rocks of Mississippian age; and (3) carbonate rocks of Pennsylvanian and Permian age (fig. 3). The total stratigraphic thickness of this unit is about 29,000 ft in the Schell Creek Range and Confusion Range on the west and east sides, respectively, of the study area (Stratigraphic Committee of the Eastern Nevada Geological Society, 1973). An oil exploration well drilled in 1983 in southern Snake Valley (fig. 4) penetrated nearly 12,000 ft of this hydrogeologic unit. The hole penetrated Ely Limestone and Chainman Shale at depths of 1,250 and 2,450 ft, respectively. Abrupt increases in borehole diameter and sonic travel time both indicate the presence of several zones of high porosity in this sequence of carbonate rocks (fig. 4). The thick sequences of carbonate rocks can be very permeable as a result of fracturing and subsequent solution widening of fractures. These rocks frequently function as regional aquifers in the eastern Great Basin. Perennial streams are absent in drainage basins underlain by carbonate rocks because these rocks are sufficiently permeable for precipitation to infiltrate.
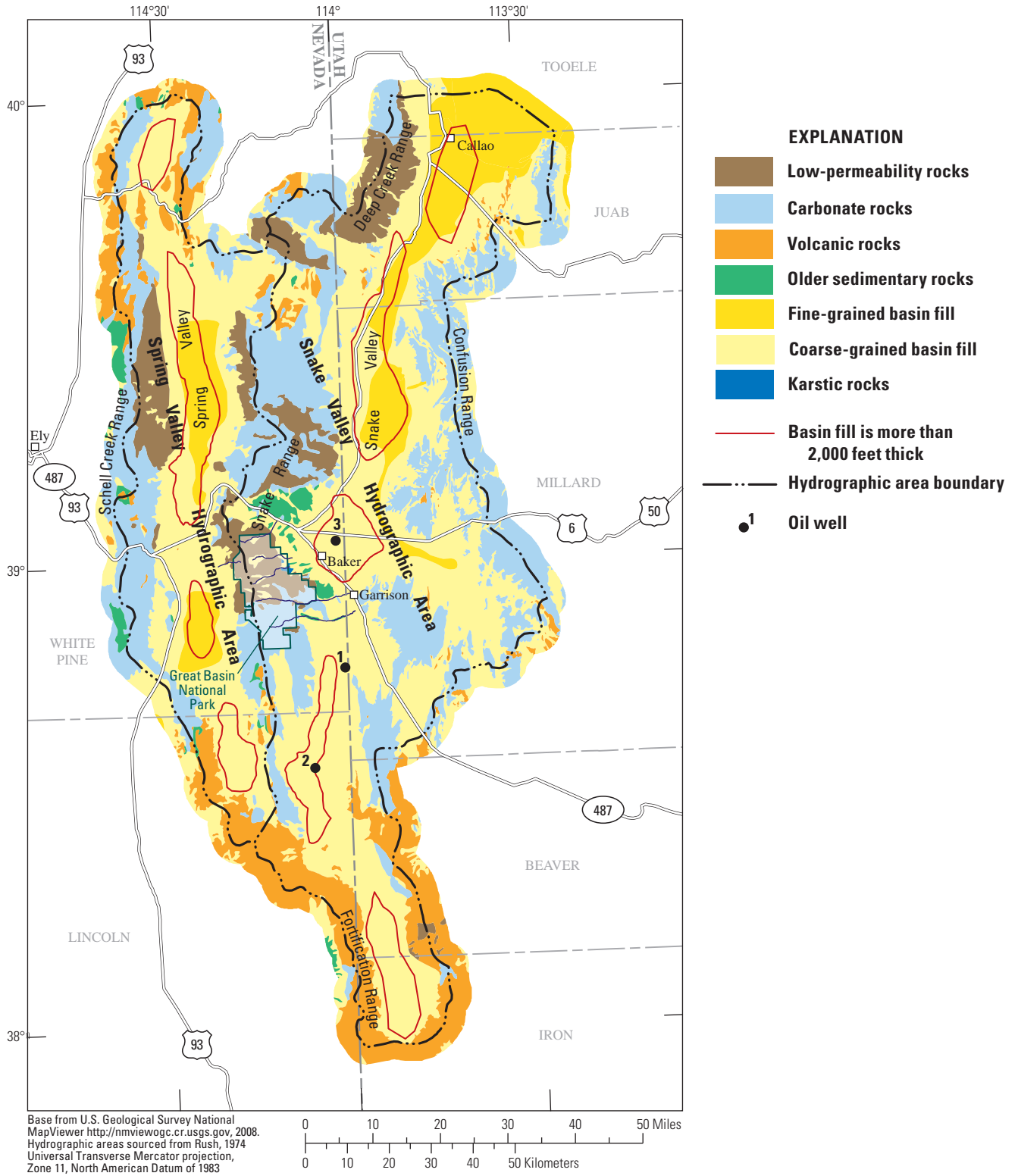
Figure 2. Surface geology and thickness of basin fill in Spring and Snake Valleys, Nevada and Utah.

Series	Hydrogeologic unit	Approximate thickness, in feet	Lithology	Simplified hydrogeologic units / Aquifers	Model layer
Quaternary to Tertiary	Younger basin-fill deposits	0 to less than 500 feet	Unconsolidated to poorly cobsolidated clay, silt, sand, gravel, and boulders of alluvial fans, basin lowlands, and stream flood plains.	Fine-grained basin fill Coarse-grained basin fill	1–3
Quaternary to Tertiary	Volcanic rocks	500 to 3,000 feet	Flows, shallow intrusives, ash-flow tuffs. Compositions range from basalt to rhyolite.	Volcanic rocks	1–4
Tertiary	Older basin-fill deposits	Less than 1,000 to more than 2,000 feet	Tuffaceous conglomerate, siltstone, mudstone, and limestone. Typically contains interbedded volcanic rocks.	Fine-grained basin fill Coarse-grained basin fill	3
Tertiary to Jurassic	Granitic rocks	More than 2,000 feet[1]	Granodiorite and quartz monzonite.	Low permeability rocks	1–4
Triassic to Cambrian	Siliceous sedimentary rocks	More than 2,000 feet[1]	Chert, siliceous shale, siltstone, sandstone, quartzite, and conglomerate.		
Permian to Cambrian	Clastic sedimentary rocks	More than 2,000 feet[1]	Conglomerate, sandstone, quartzite, and shale.		
Devonian to Cambrian	Carbonate rocks	More than 2,000 feet[1]	Limestone and dolomite with subordinate sandstone and shale.	Carbonate rocks Karstic rocks	1–4

[1] Total model thickness is 2,000 feet.

Figure 3.   Hydrogeologic units, thickness, lithology, aquifer, and model layers of series in southern Spring and Snake Valleys, Nevada and Utah.

Figure 4. Lithologic and geophysical logs for oil exploration well number 1 (API 27-033-05245), Snake Valley, Nevada. (Location of oil exploration well is shown in figure 2.)

Karstic rocks occur near the eastern boundary of Great Basin National Park and host caves such as Lehman Cave (National Park Service, 2007). These karstic rocks locally affect surface-water and groundwater flow between Baker and Lehman Creeks. Baker Creek loses 2,900 acre-ft/yr (4 ft^3/s) and Lehman Creek gains 2,200 acre-ft/yr (3 ft^3/s) along the reaches that bound Lehman Caves and Rowland Spring (Elliott and others, 2006).

The volcanic rocks consist of ash-flow tuffs of rhyolite-to-andesite composition exposed in mountainous southern parts of the study area and basalt, andesite, and rhyolite lava flows in mountainous northern parts (Sweetkind and others, 2007, p. 30). Oil exploration well number 2 that was drilled in Southern Snake (Hamlin) Valley (figs. 2 and 5) penetrated tuff at depths of 3,470–4,100 ft. Oil exploration wells number 1 (fig. 4) and number 3 (fig. 6) that were drilled farther north in Snake Valley (fig. 2) penetrated basin-fill deposits and underlying rocks of Paleozoic age and did not penetrate any volcanic rocks. Oil exploration wells numbers 1, 2, and 3 (fig. 2) have Nevada Bureau of Mines and Geology (2008) API numbers: 27-033-05245, 27-017-05223, and 27-033-05288, respectively. Sweetkind and others (2007, p. 31) have inferred subsurface thicknesses of 500–8,000 ft of tuff in southern parts of the study area. Hydraulic conductivity of volcanic rocks can range over several orders of magnitude. High values probably represent fractured volcanic-rock aquifers, and low values represent volcanic rocks that function as confining units (Sweetkind and others, 2007, p. 32).

Older sedimentary rocks of Miocene age are exposed along the west margin of Snake Valley from the southern end of the northern Snake Range to the southern Snake Range several miles south of Baker, Nevada (fig. 2). Where exposed, these rocks comprise west dipping cemented fine-grained lacustrine deposits and coarse-grained sandstone and conglomerate (Sweetkind and others, 2007, p. 28). They are thought to be present at uncertain depth beneath younger basin-fill deposits. They include evaporite deposits of anhydrite and gypsum (figs. 5 and 6) and an uncertain thickness of overlying rock that underlies younger basin fill. These rocks probably function as a low permeability interval between younger basin-fill deposits (basin-fill aquifers) and Paleozoic carbonate rocks at depth.

Coarse-grained and fine-grained basin fill of Holocene to Pliocene age underlie alluvial fans and basin lowlands in Spring and Snake Valleys (fig. 2). The alluvial fans comprise poorly sorted mixtures of sand and gravel and, in close proximity to mountain fronts, increasing proportions of cobbles and boulders. Toward basin lowlands these deposits consist of sand and gravel. The basin-fill aquifers are found in these deposits.

The fine-grained basin fill comprises, silt, and clay of Holocene to Pliocene age that accumulated in a playa in Spring Valley and in Lake Bonneville in Snake Valley (Sweetkind and others, 2007, p. 30). These deposits underlie the lowest parts of basins and function as confining units between shallow water table and deeper confined aquifers that consist of coarse-grained basin-fill deposits. Fine-grained basin fill and coarse-grained basin fill probably complexly interfinger where they meet near the margins of basin lowlands.

Loose uncemented sand and gravel deposits are indicated by borehole washouts in all caliper and sonic logs where the lithologic log reported unconsolidated basin fill (figs. 4–6). This evidence includes abrupt increases in hole diameter and sonic travel time. Washouts are evident especially at 500–600 and 1,240–1,400 ft in oil well number 3 (fig. 6).

Geophysical and lithologic logs show low permeability material occurs at depths greater than 1,600 ft below land surface in oil well numbers 2 and 3. Borehole diameter increases gradually at depths below 2,150 ft and increases abruptly at a depth of 2,300 ft in oil well number 2 (fig. 5). This indicates that a more soluble evaporite underlies the 500-foot thick anhydrite sequence. Dissolution of an evaporite also would decrease resistivity and increase sonic travel time. The lithologic change from unconsolidated basin fill to clay at 1,400 ft below land surface in oil well number 3 is inconsistent with increasing resistivity and decreasing sonic travel time (fig. 6). The geophysical logs indicate shale was encountered rather than clay, but the permeability is low for either clay or shale.

Groundwater flow through basin fill occurs at depths less than 2,000 ft in Snake Valley south of U.S. Highway 50 (fig. 2). Basin fill that is thicker than 2,000 ft covers less than 30 percent of Snake Valley. Deeper sediments predominantly are low permeability rocks where the thickness of basin fill exceeds 2,000 ft.

Figure 5. Lithologic and geophysical logs for oil exploration well number 2 (API 27-017-05223), Snake Valley, Nevada. (Location of oil exploration well is shown in figure 2.)
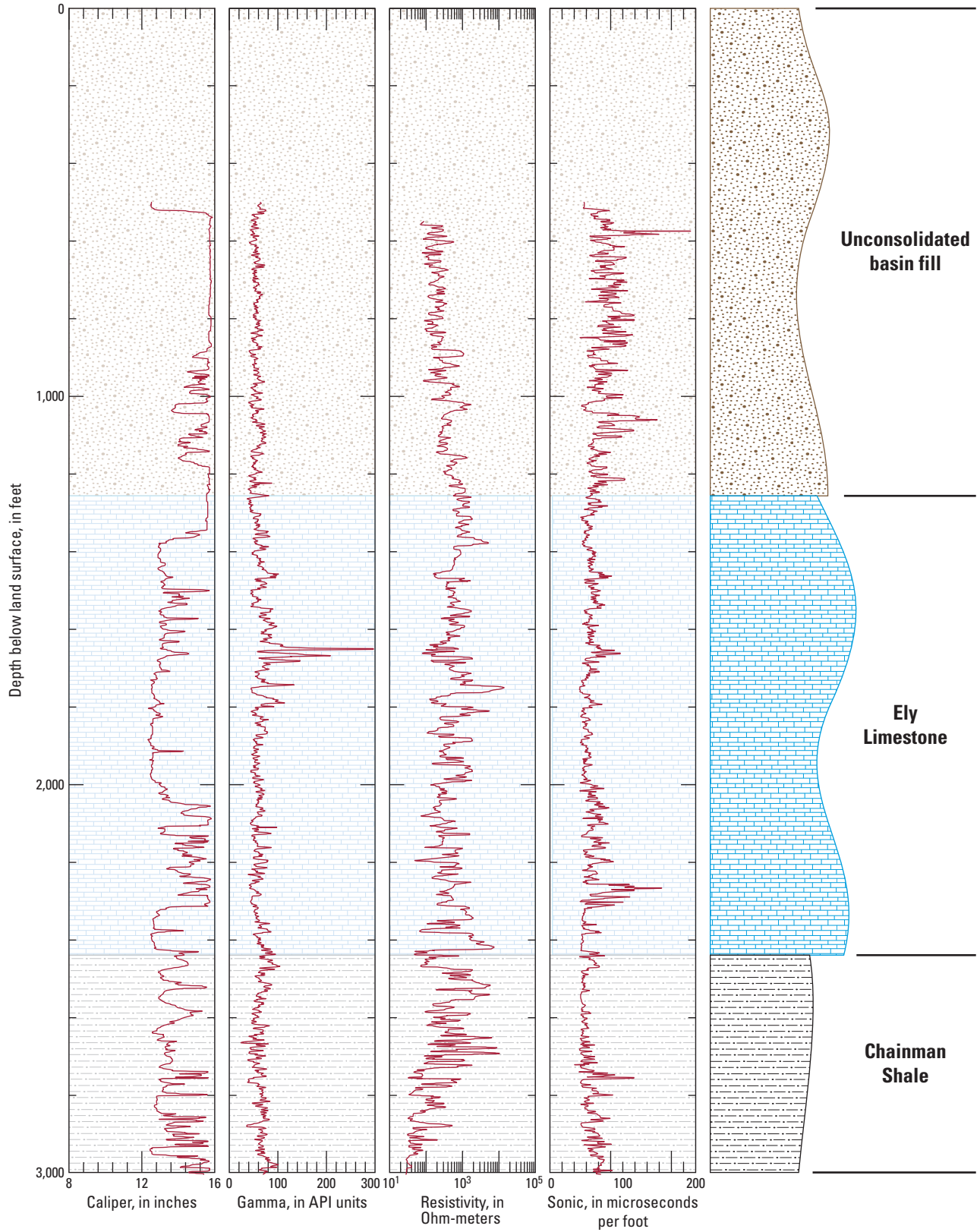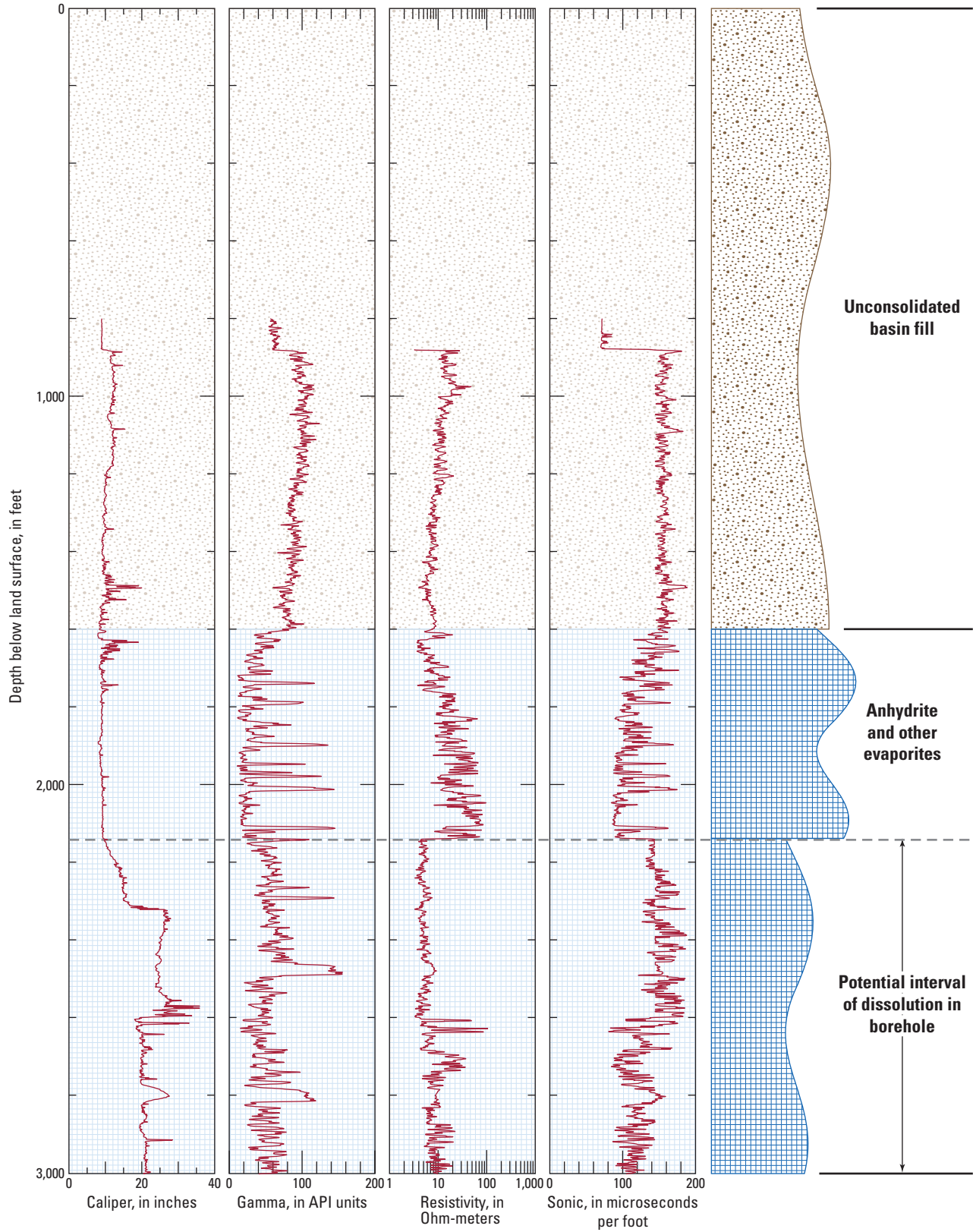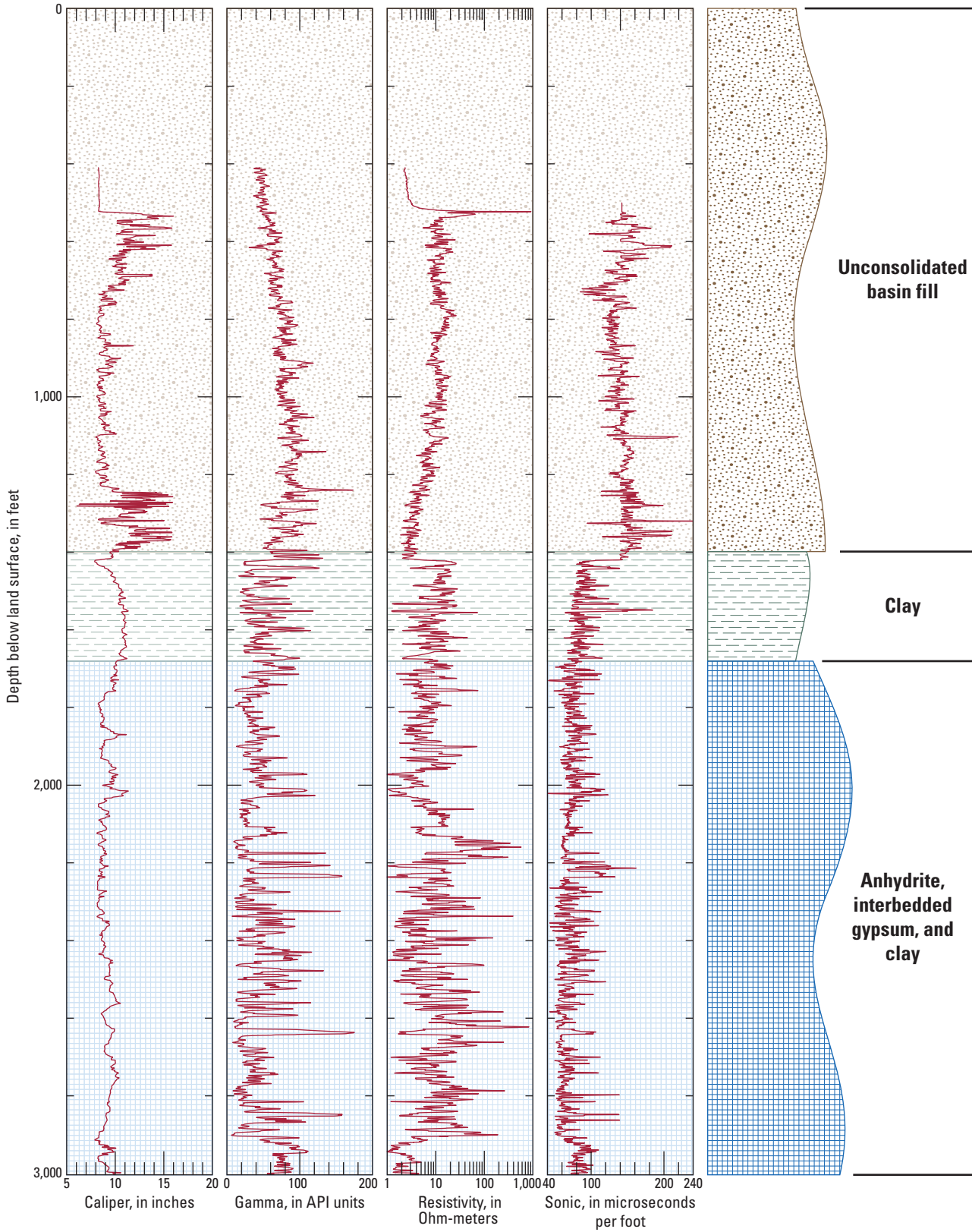
Figure 6.   Lithologic and geophysical logs for oil exploration well number 3 (API 27-033-05288), Snake Valley, Nevada. (Location of oil exploration well is shown in figure 2.)

Hydraulic Properties

The hydraulic properties of basin fill, carbonate rock, and volcanic rocks were estimated from eight aquifer tests in Lake, Spring, and Snake Valleys (fig. 7). Transmissivity and specific yield were estimated for each aquifer test by fitting analytical or numerical groundwater-flow models to measured water-level responses. Water-level responses were analyzed for five conventional aquifer tests where a single well was pumped for less than 1 week. The maximum volume pumped during a conventional aquifer test did not exceed 40 acre-ft (table 1). Water-level responses to multiple years of irrigation pumping were analyzed for three "irrigation" aquifer tests. The volumes of pumped water were more uncertain, but minimum volumes ranged from 10,000 to 210,000 acre-ft (table 1). Transmissivities of basin fill have been estimated from other aquifer tests in the study area (Ertec Western, Inc., 1981; Leeds, Hill and Jewett, Inc., 1981, 1983; Bunch and Harrill, 1984).

Ranges of transmissivity and specific yield of basin fill and carbonate rock were estimated using irrigation aquifer test results by analyzing water-level changes in multiple observation wells that were caused by groundwater pumping for irrigation (table 1). Water-level declines during the 2000–03 irrigation seasons were analyzed in Snake Valley because crops had been inventoried (Welborn and Moreo, 2007) and drought conditions existed during this period. Hydraulic properties were estimated by minimizing a weighted sum-of-squares objective function that compared simulated and measured drawdowns (Halford, 2006). Seasonal drawdowns from spatially distributed groundwater pumping were simulated with a three-dimensional, MODFLOW model.

Ranges of transmissivity and specific yield were estimated with the irrigation aquifer tests because groundwater withdrawals were uncertain. Annual pumping estimates were computed as the product of irrigated acreage and annual consumptive use, which was annual application minus return flow. Irrigated acreage in Snake Valley was estimated from crop inventories and satellite imagery during 2000, 2002, and 2005 (Wellborn and Moreo, 2007). Irrigated acreage in Lincoln County from 1963 through 2008 was estimated from well logs, crop inventories, and satellite imagery (Southern Nevada Water Authority, 2009) using methods from Moreo and others (2003). Annual consumptive use was estimated to the nearest foot so annual consumption was either 2 or 3 ft (U.S. Geological Survey, 2010). An annual consumptive use of 2 ft was more likely where surface water was available.

Hydraulic-property estimates from aquifer tests represent an integrated average through an area and thickness of aquifer. The volume of aquifer investigated reasonably can be defined and compared by a drawdown threshold. This threshold is defined by the error associated with the drawdown estimates which were about 0.1 and 1 ft for conventional and irrigation aquifer tests, respectively. The drawdown threshold for conventional aquifer tests is smaller than for irrigation aquifer tests, because water levels were measured continuously and minimally affected by environmental noise. Areal extent and volume of investigated aquifer become nearly proportional as the volume of water pumped increases. This is because aquifer thickness becomes "small" relative to the affected area.

Hydraulic-property estimates from the conventional aquifer tests were more certain than from the irrigation aquifer tests but represented less than 500 acres. This is because the uncertainty of the volume pumped during conventional aquifer tests was less than 10 percent. The maximum volume pumped during conventional aquifer tests was 40 acre-ft (table 1).

Hydraulic-property estimates from the irrigation aquifer tests were less certain than from the conventional aquifer tests but represented areas of more than 50,000 acres. Hydraulic-property estimates were less certain because the uncertainty of the volume pumped during irrigation aquifer tests was about 40 percent. The volumes pumped during irrigation aquifer tests were 1,000 times more than volumes pumped during conventional aquifer tests (table 1). Differences in annual consumptive use affected transmissivity and specific-yield estimates, but the area where drawdowns exceeded 1 ft did not change.

Transmissivity of the basin fill ranged from 1,200 to 13,000 ft^2/d where basin fill thickness exceeded 1,000 ft (table 1). The average hydraulic conductivity of the coarse-grained, basin fill was 3 ft/d and the fine-grained, basin fill was 0.1 ft/d. Specific yield of the basin fill volumetrically averaged 15 percent and ranged from 12 to 18 percent from the irrigation aquifer tests. Vertical-to-horizontal anisotropy could not be estimated and was assumed to be 0.1.

Transmissivity of the carbonate rocks ranged from 7,000 to 55,000 ft^2/d (table 1). Specific yield of the carbonate rocks averaged 2 percent and ranged from less than 1 to 4 percent. Vertical-to-horizontal anisotropy of the carbonate rocks ranged from 0.2 to 1 at sites W101, W103, and W105.

Hydraulic conductivity of granitic, intrusive, volcanic, and other low-permeability rocks rarely exceeded 0.1 ft/d. These rocks typically restrict groundwater flow. Site W508M was the only well in low-permeability rocks that was tested in the area of interest and the transmissivity of the volcanic rocks was 70 ft^2/d (table 1; Southern Nevada Water Authority, 2009). Hydraulic conductivity averaged 0.06 ft/d across the well-screen interval at site W508M. Hydraulic conductivity averaged 0.01 ft/d in wells UE-19i and UE-20f at the Nevada Test Site (Blankennagel and Weir, 1973), which is about 100 mi northwest of Las Vegas (fig. 1). These wells penetrated more than 20,000 ft of partially welded tuff, rhyolytic lava, and bedded tuff. Hydraulic conductivity of granitic rocks in wells U-15k, ER-8-1, and U-12s at the Nevada Test Site are 0.0000001, 0.000002, and 0.006 ft/d, respectively.
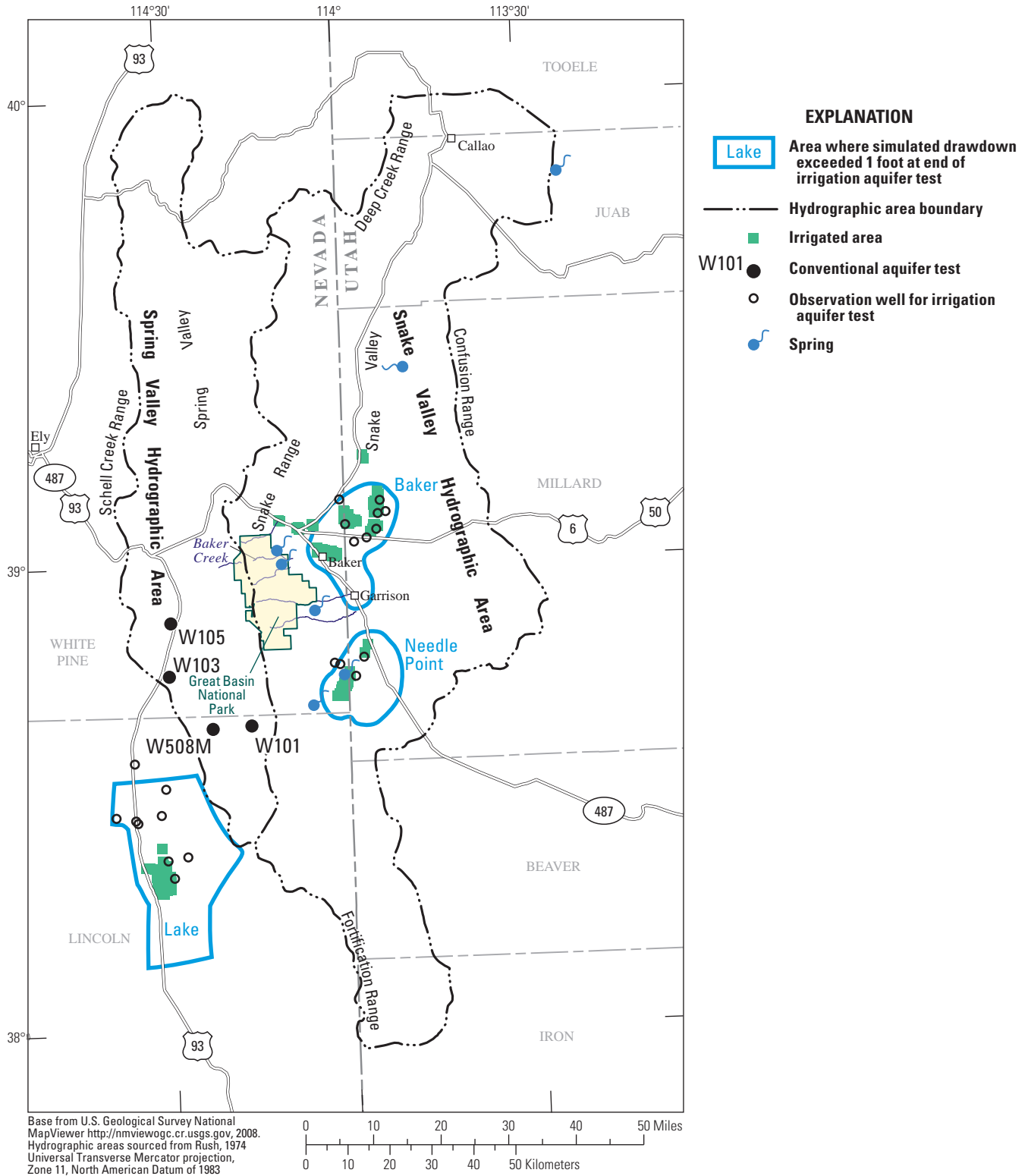
Figure 7. Aquifer test locations and investigated areas, Nevada and Utah.

Table 1.   Hydraulic properties estimated from eight aquifer tests, Nevada and Utah.

[Data from U.S. Geological Survey (2010), accessed February 14, 2010, at http://nevada.usgs.gov/water/aquifertests/index.htm. Site locations are shown in figure 7. acre-ft, acre-foot; ft²d, square foot per day. na, not applicable]

Site	Lithology	Observation wells	Volume pumped (acre-ft)		Transmissivity (ft²/d)		Specific yield	
			Minimum	**Maximum**	**Minimum**	**Maximum**	**Minimum**	**Maximum**
Irrigation aquifer tests								
Lake	Basin fill	9	210,000	310,000	9,000	13,000	0.12	0.18
Baker	Basin fill	8	31,000	46,000	5,600	9,000	0.12	0.18
Needle Point	Basin fill	4	10,000	15,000	1,200	1,300	0.12	0.13
	Carbonate rock	4	10,000	15,000	7,000	16,000	0.001	0.006
Conventional aquifer tests								
Baker Creek	Basin fill	4	0.4		800		0.05	
W101	Carbonate rock	1	33		10,000		0.02	
W103	Carbonate rock	1	7		10,000		0.04	
W105	Carbonate rock	1	40		55,000		0.04	
W508M	Volcanic rock	0	0.1		70		na	

Estimation of Hydraulic Property Distributions with Numerical Models

The hydraulic conductivity of basin fill and transmissivity of basement rock distributions in Spring and Snake Valleys were refined by calibrating a steady state, three-dimensional, numerical groundwater-flow model of the carbonate-rock province to predevelopment conditions. Hydraulic properties and boundary conditions were defined primarily from the RASA model (Prudic and others, 1995) except in Spring and Snake Valleys. This locally refined model will be referred to as the Great Basin National Park calibration (GBNP-C) model. Groundwater flow through the study area was simulated with the modular finite-difference model MODFLOW (Harbaugh and others, 2000).

Refinement of RASA Model

The GBNP-C model was divided areally into 230 rows of 184 columns of variably spaced, rectangular cells (fig. 8). The smallest cells were 1,640 ft on a side, square cells that encompassed the Great Basin National Park. This 1.1 million acre area was divided into 152 rows of 122 columns. Cell lengths and widths were multiplied successively by 1.2 away from the area of uniform small cells. A maximum cell dimension of 39,000 ft was specified so the largest GBNP-C model cells would not contain more than one of the original RASA nodes. The model grid was oriented north-south in UTM, zone 11, NAD83 projection for convenience.

The GNBP-C model was divided vertically into four layers that extended below the average water table under predevelopment conditions. Layer 1 was 10 ft thick to better simulate groundwater/surface-water interaction. Layer 2 was

50 ft thick to better define extensive fine-grained deposits in Snake Valley (Reheis, 1999) that affected water-level responses to irrigation pumping near Baker, Nevada. Layers 1 and 2 were active only in Spring and Snake Valleys and were added primarily to simulate surface-water features with limited subsurface penetration. The water table occurred at the top of layer 3 outside of Spring and Snake Valleys. Layer 3 primarily simulated basin fill more than 60 ft thick in Spring and Snake Valleys (Watt and Ponce, 2007) and the full thickness of basin fill beyond Spring and Snake Valleys. Layer 4 simulated basement rocks through the entire study area. The thicknesses of layers 3 and 4 were variable and ranged from 1 to 2,000 ft.

Minimal groundwater flow was expected at depth so the thickness of basin fill in layer 3 was limited to 2,000 ft. Groundwater flow tends to diminish with depth in isotropic, homogeneous aquifers (Tóth, 1962) but could be significant at depth in an anisotropic, heterogeneous aquifer if the most transmissive units were at depth (Freeze and Witherspoon, 1967). The hydraulic conductivity of the heterogeneous basin fill in Spring and Snake Valleys generally decreases with depth because of increased cementation, induration, and occurrence of evaporative deposits (Welch and others, 2007). Unconsolidated coarse-grained younger sedimentary rocks occur in the upper 2,000 ft and become indurated with depth. These deposits generally are underlain by Miocene sediments that contain thick anhydrite in southern Snake Valley (fig. 5).

Nominal thicknesses were assigned to layer 4 primarily for drawing sections and were not used to define the transmissivity of the basement rocks. Thickness of the basement rocks in layer 4 was assigned so the thickness of layers 3 and 4 totaled about 2,000 ft. Thicknesses in layer 4 also were used to extrapolate hydraulic conductivity where basement rocks occurred at the water table.

Figure 8.   Finite-difference grid and lateral boundaries for the RASA and GBNP-C models, Spring and Snake Valleys, Nevada and Utah.

Hydraulic Properties

All hydraulic properties in the GBNP-C model were defined through the Block Centered Flow (BCF) package (McDonald and Harbaugh, 1988) to m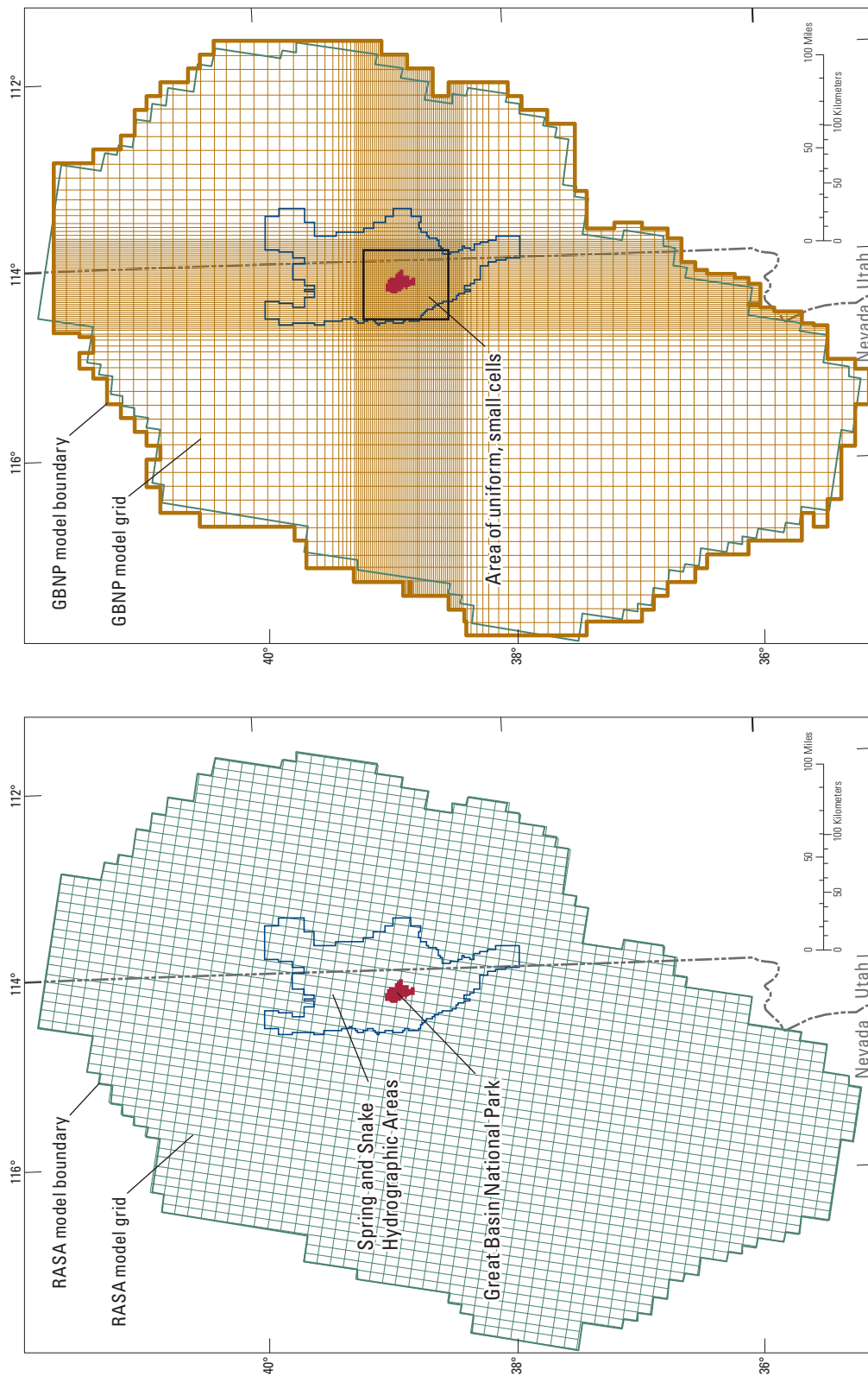aintain continuity with the RASA model. Transmissivity of layers and vertical leakance between layers are specified directly in the BCF file so corresponding layer thicknesses were not developed for the RASA model. Transmissivity and vertical leakance of active layers outside of Spring and Snake Valleys were interpolated directly from the RASA model (Prudic and others, 1995) and were not changed during model calibration. All hydraulic properties were assumed laterally isotropic throughout the entire model.

Hydraulic conductivity and transmissivity were distributed throughout Spring and Snake Valleys with pilot points, which are mapped locations where hydraulic properties were assigned (RamaRao and others, 1995). A total of 416 pilot points were used with 104 mapped locations that were projected through all four model layers. Hydraulic properties were interpolated from pilot points to model cells with kriging (Doherty, 2008b). Interpolation occurred within the basin-fill, carbonate-rock, karst, and low-permeability hydrogeologic units. Pilot-point density was greatest around Great Basin National Park in Snake Valley (figs. 1 and 9). Pilot points were at aquifer-test sites so hydraulic-property estimates could be specified.

The spatial variability of hydraulic conductivity and transmissivity was defined with variograms of basin fill, basement rocks, and karst. All variograms were exponential, applied to log-transformed properties, and estimated the assigned value at each pilot point, nugget = 0 (Isaaks and Srivastava, 1989). The basin-fill and basement-rocks variograms had a 2:1 anisotropy where the major axes were aligned with the trough of Snake Valley for interpolation of properties north of U.S. Highway 50 and a range of 60 mi along the major axis. Karst was defined with a third variogram with a 4:1 anisotropy where the major axis paralleled the losing reach of Baker Creek and the gaining reach of Lehman Creek. The range of the karst variogram was 5 mi because the extent was limited to the area around Lehman Caves (fig. 9).

Hydraulic conductivity of the basin fill, layers 1, 2, and 3, was estimated during model calibration because transmissivity is affected strongly by changes in saturated thickness near the edge of unconsolidated sediments. Hydraulic conductivity was interpolated between coarse-grained and fine-grained units because a gradational change between units was conceptualized. Average hydraulic conductivities of the coarse-grained units in Snake Valley were 1–5 ft/d and about 20–30 times greater than the hydraulic conductivities of the fine-grained units (table 1).

Transmissivity of the basement rocks was estimated because hydraulic conductivity is highly variable and thickness is correlated poorly with transmissivity. This finding resulted from extensive testing of the lower carbonate aquifer around the Nevada Test Site (Winograd and Thordarson, 1975, p. C20). The observations of Winograd and Thordarson (1975) were,

> "None of the eight holes drill-stem tested showed a uniform pattern of increase or decrease in fracture transmissibility, and open fractures were present as much as 1,500 feet beneath the top of the aquifer and 4,200 feet below land surface. In some holes the transmissibility increased markedly with depth; in others the most permeable zones were near the top of the zone of saturation."

Hydraulic-property estimates were limited to a single value per hydrogeologic unit at the mapped location of each pilot point (fig. 10). Between 1 and 3 hydraulic properties were estimated at each mapped location. Coarse-grained basin-fill was assumed to have the same hydraulic conductivity at a mapped location regardless whether any intervening fine-grained basin-fill was present in layer 2. Hydraulic conductivity of basement rocks in layers 1–3 was calculated from transmissivity estimates in layer 4 so consistent hydraulic properties could be specified in the mountain blocks. A hydraulic conductivity that is specified from estimates in deeper layers will be discussed herein as "tied".

Hydraulic properties were specified and not estimated at 228 of the 416 pilot points in Spring and Snake Valleys (table 2). About 80 percent of these values were specified because the hydraulic conductivity was tied to hydraulic-property estimates in deeper layers. The remaining specified values were aquifer-test results (table 1). Assigned hydraulic-conductivity estimates in basin fill were transmissivity estimates from aquifer tests divided by the simulated thickness of basin fill in the GBNP-C model. Aquifer-test results were specified because transmissivity estimates are known within a factor of 2. This is a minor degree of variability relative to the uncertainty in transmissivity values that were estimated through regional model calibration. Potential variability in hydraulic conductivity of the basin fill was reduced artificially where results from the Baker irrigation analysis were assigned to two mapped locations in the basin fill.

Continuity with the remainder of the RASA model area was maintained with 188 additional pilot points that surrounded Spring and Snake Valleys (fig. 9). These pilot points occupied 94 mapped locations in layers 3 and 4. Transmissivity estimates were sampled from the RASA model (Prudic and others, 1995), assigned to these pilot points, and not changed during calibration of the GBNP-C model.

Vertical hydraulic conductivity in Spring and Snake Valleys was assumed 0.1 of lateral hydraulic conductivity. Vertical leakance values were computed from estimated hydraulic conductivity distributions for each layer and have units of feet per day per foot (d^{-1}).
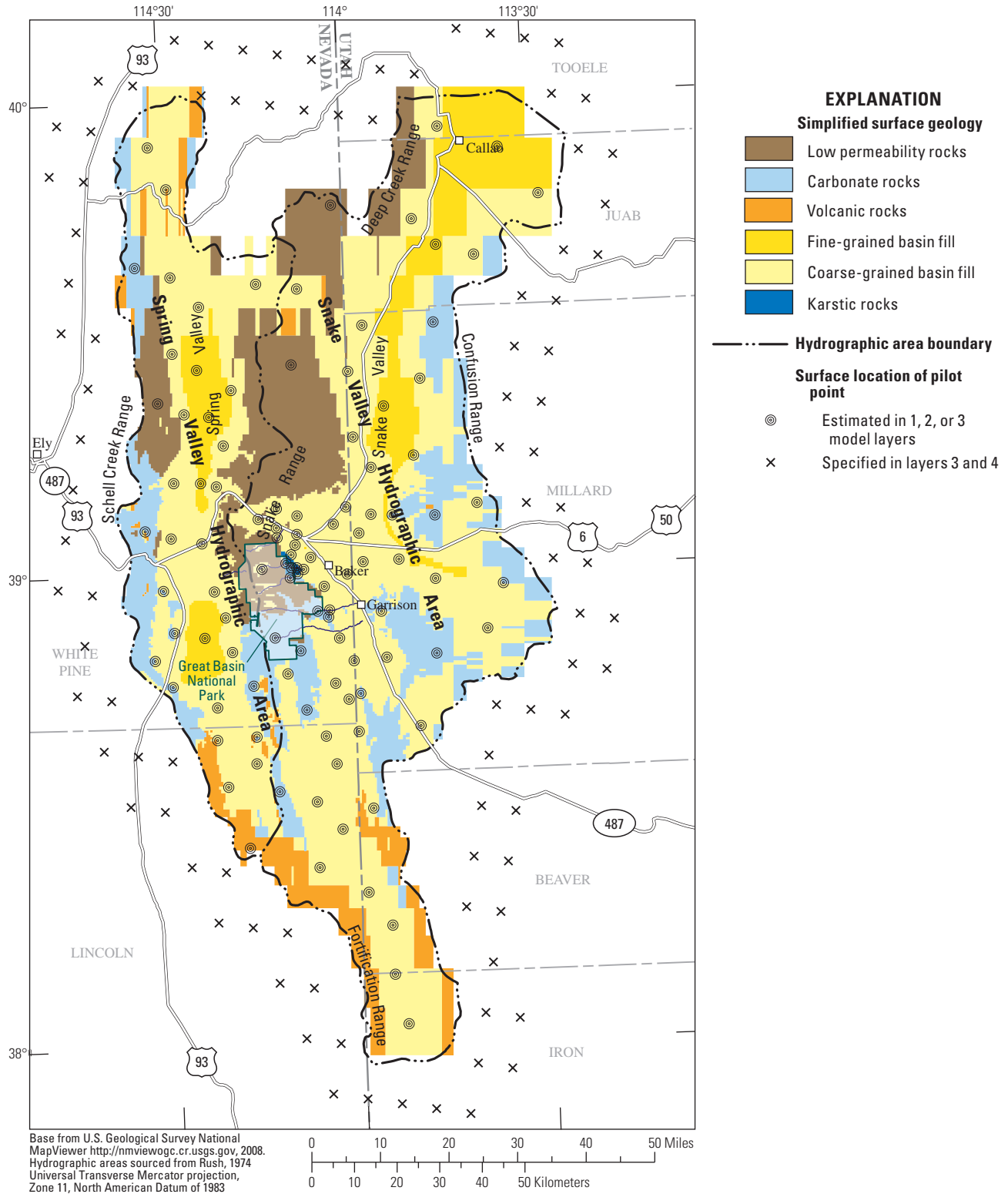
Figure 9.   Simplified surface geology and mapped pilot points for interpolation of hydraulic conductivity or transmissivity, Spring and Snake Valleys, Nevada and Utah.
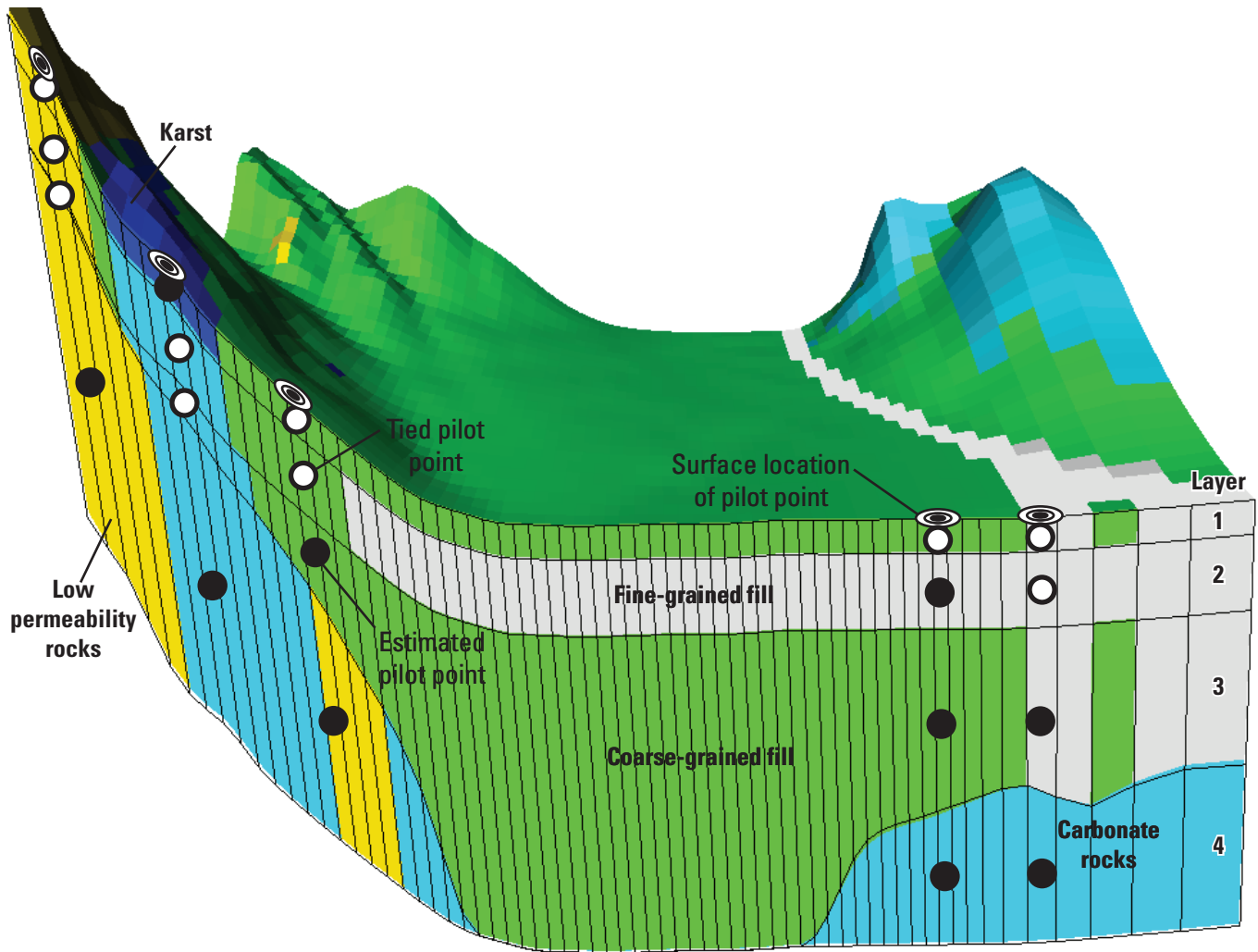
Figure 10. Example of distributing pilot points vertically and constraining hydraulic-property estimates to a single value per mapped location.

Table 2. Distribution of pilot points for estimating hydraulic conductivity and transmissivity by model layer and hydrogeologic unit, Spring and Snake Valleys, Nevada and Utah.

[–, no pilot points]

Simplified hydrogeologic unit	Hydraulic conductivity pilot points						Transmissivity pilot points	
	Layer 1		Layer 2		Layer 3		Layer 4	
	Estimated	Specified	Estimated	Specified	Estimated	Specified	Estimated	Specified
Low permeability rocks	–	4	–	5	–	9	25	6
Carbonate rocks	–	15	1	14	–	22	52	15
Volcanic rocks	–	1	–	1	–	1	3	3
Fine-grained basin fill	–	6	24	9	6	–	–	–
Coarse-grained basin fill	2	71	5	40	60	6	–	–
Karstic rocks	5	–	5	–	–	–	–	–

Recharge

Recharge mostly occurs through the alluvial fans and carbonate mountain blocks in Spring and Snake Valleys. Precipitation in excess of local evapotranspiration (ET) is available for infiltration and surface runoff on mountain blocks. Most of the mountain blocks are underlain by low-permeability bedrock that limits local infiltration and directs runoff to alluvial fans where it infiltrates. Recharge from runoff to the valley floors was assumed negligible and not simulated.

Recharge areas are herein classified as mountain block and mountain front where recharge, regardless of area, refers to water that has infiltrated deeper than the root zone and migrated through the unsaturated zone to the water table. Mountain-block recharge is precipitation that infiltrated bedrock in the mountains. Mountain-front recharge is surface runoff that is routed through streams and unmapped channels and infiltrates through basin fill.

Mountain-Block Recharge and Mountain-Front Recharge

Mountain-block recharge primarily occurs where permeable carbonate rocks are exposed and to a much lesser extent through granitic, intrusive, volcanic, and other undifferentiated low-permeability rocks. Recharge to permeable, carbonate rocks was simulated as spatially variable specified flow rates and assigned with the MODFLOW recharge package. Recharge in low-permeability rocks was simulated with specified heads because recharge rates vary widely across mountain blocks, but are all small quantities relative to other recharge terms. Heads were specified at the bottom of drainages where perennial streams occurred. Flow rates were constrained by average hydraulic conductivities of 0.0002 ft/d in the low-permeability rocks.

Mountain-front recharge represented net infiltration of surface runoff from mountain blocks onto alluvial fans that primarily occurred within a few miles of the contact between mountain block and basin fill. Mountain-front recharge does not differ conceptually from stream recharge. Subsurface flow between the mountain block and basin fill is not a component of mountain-front recharge and was simulated as a separate component of flow.

Recharge Distribution

A potential recharge distribution was estimated from available precipitation—where available precipitation is the annual precipitation minus 9.5 in. Annual precipitation was defined by the 1971–2000 PRISM distribution (Daly and others, 1994; PRISM Group, 2006). A minimum, annual precipitation threshold of 9.5 in. was specified because the volume of annual precipitation in excess of 9.5 in. totaled 240,000 acre-ft. This volume equals the annual groundwater discharge from Spring Valley, Snake Valley, and Fish Springs (Welch and others, 2007). A minimum, annual-precipitation threshold of 8 in. was specified previously by Maxey and Eakin (1949), but in relation to the Hardman (1936) precipitation distribution.

Accumulating the volume of precipitation above a precipitation threshold differs from accumulating volumes of precipitation for estimating recharge with Maxey and Eakin (1949). Maxey-Eakin recharge estimates sum the entire volume of precipitation between two contour intervals and reduce the volume with an efficiency coefficient. Precipitation-threshold recharge estimates sum the volume in excess of the threshold, but an efficiency coefficient is not applied. Maxey-Eakin style precipitation volumes before multiplying by efficiency coefficients are about triple precipitation-threshold volumes for a precipitation threshold of 9.5 in. in Spring and Snake Valleys.

Precipitation on the valley floor of Hamlin Valley in southern Snake Valley was excluded from available precipitation because annual PRISM estimates were deemed anomalous—greater than 20 in. These estimates of annual precipitation seemed excessive because vegetation in Hamlin Valley is similar to non-phreatophytic vegetation elsewhere in Snake Valley where annual precipitation is less than 8 in. Annual precipitation likely was overestimated by PRISM because most of the floor of Hamlin Valley occurs at altitudes greater than 6,000 ft above sea level.

Potential recharge rates were the volume of available precipitation accumulated in 1 of 63 recharge zones divided by the infiltrating area of a zone. The recharge zones resulted from dividing Spring and Snake Valleys into 18 rows from north to south and splitting each valley into eastern and western halves (fig. 11). The east-west subdivision of each valley was the thalweg as defined by the minimum land-surface elevation along each GBNP-C model row. Western zones in Snake Valley near U.S. Highway 50 were subdivided further (fig. 11). The infiltrating area of a zone extended from 300 ft above the thalweg to the mountain divide. Areas that were mapped as low-permeability rocks or without surface channels were excluded from the infiltrating area. Areas without surface channels were defined by model cells where the length of mapped channels in a cell divided by the square-root of cell area was less than 0.25.

Recharge was distributed throughout Spring and Snake Valleys with pilot points (RamaRao and others, 1995). A total of 209 pilot points were used in layer 1 (fig. 11). Recharge rates were interpolated from pilot points to model cells with kriging (Doherty, 2008b). Interpolation occurred independently within the basin-fill, carbonate-rock, and low-permeability hydrogeologic units (fig. 9). Pilot-point density was greatest around GBNP in Snake Valley (fig. 11).
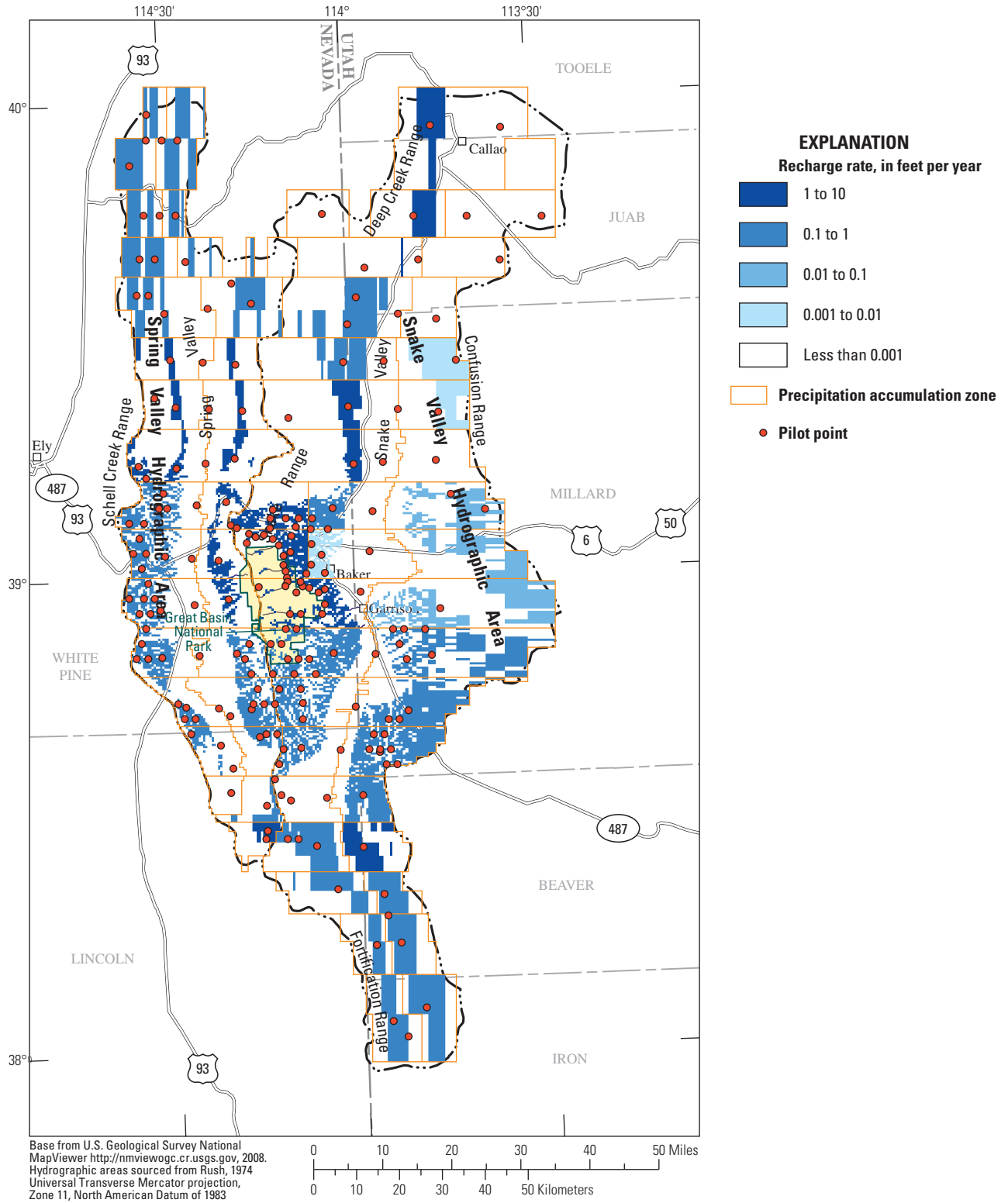
Figure 11.   Potential recharge and mapped pilot points for distributing recharge rates in the GBNP-C model.

The spatial variability of recharge was defined with variograms of basin fill and basement rocks. All variograms were exponential, applied to log-transformed recharge rates, and would estimate the assigned value at each pilot point, nugget = 0 (Isaaks and Srivastava, 1989). The basin-fill variogram had a 2:1 anisotropy where the major axis was aligned with the axis of the valleys, a bearing of 10°, and a range of 40 mi along the major axis. The basement-rocks variogram was isotropic with a range of 30 mi and applied to the carbonate-rock and low-permeability hydrogeologic units.

Initial pilot-point values were sampled directly from the potential recharge distribution (fig. 11). An initial annual rate of 0.0001 ft was assigned to pilot points mapped over low-permeability hydrogeologic units. Fixed values of zero were assigned on the valley floors where steep recharge-rate gradients existed between mountain front and valley floor. Pilot-point values on the valley floor were assigned and not estimated.

Recharge to the remainder of the GBNP-C model outside of Spring and Snake Valleys was distributed as specified in the original RASA model (Prudic and others, 1995). Annual recharge outside of Spring and Snake Valleys totaled 1,342 and 1,341 thousand acre-ft in the GBNP-C and RASA models, respectively. Minor differences existed because of the differences in grid resolutions and rotation.

Groundwater Discharge

Groundwater discharged from the surfaces of Spring and Snake Valleys by evapotranspiration and spring discharge prior to development. Evapotranspiration (ET) is a process by which shallow groundwater is either evaporated from soils or transpired by plants. Spring discharge ultimately evapotranspires from the valleys so spring discharge is included in remote-sensing estimates of ET (Smith and others, 2007; Welch and others, 2007, p. 50).

The predevelopment distribution and annual rates of groundwater discharge from Spring and Snake Valleys have been mapped and quantified (fig. 12). Groundwater discharge generally occurred across valley floors where playa, phreatophytic vegetation, marsh, meadow, and open water were present (Smith and others, 2007). Groundwater-discharge areas were subdivided into areas of similar ET rates that are referred to as ET units. The groundwater-discharge rate from an ET unit (GW_{ET}) was the difference between annual ET and annual precipitation. Annual groundwater-discharge estimates totaled 208,000 acre-ft from Spring and Snake Valleys (Welch and others, 2007, app. A).

Big Springs, Big Springs run, and Twin Springs, which occur on the floor of Snake Valley, were simulated explicitly in the GBNP-C model. GW_{ET} rates were reduced to the average, 0.2 ft/yr, downgradient of each explicitly simulated spring or gaining reach because spring discharge was incorporated in the original estimates. Areas of reduced GW_{ET} extended downgradient until the cumulative GW_{ET} in excess of 0.2 ft/yr equaled spring discharge. For example, discharge from Big Springs and Big Springs run equaled the GW_{ET} in excess of 0.2 ft/yr from Big Springs to 2 mi north of Garrison (fig. 12). This approach was not applied to Cave, Home Farm, Kious, Rowland, and Spring Creek Springs and gaining reaches of Lehman and Strawberry Creeks because the discharges are small relative to the uncertainty of the GW_{ET} estimates (table 3).

Distributed GW_{ET} and spring discharge were simulated as specified discharges in the GBNP-C model that were simulated with the well package in MODFLOW (Harbaugh and others, 2000). Distributed GW_{ET} was sourced from model layer 1 and the specified discharge equaled cell area multiplied by the mapped GW_{ET} rate (fig. 12). Spring discharges were specified at measured rates and were sourced from layers 2, 3, or 4 (table 3).

Losses from Baker Creek and gains on Lehman Creek were simulated with specified heads in the GBNP-C model because creek stages are known better than the distribution of gains and losses. Baker Creek loses 2,900 acre-ft/yr (4 ft³/s) and Lehman Creek gains 2,200 acre-ft/yr (3 ft³/s) along the reaches that bound Lehman Caves and Rowland Spring (Elliott and others, 2006).

Groundwater discharge from the remainder of the GBNP-C model outside of Spring and Snake Valleys was simulated as specified in the original RASA model (Prudic and others, 1995). Distributed GW_{ET} was simulated with the evapotranspiration package (Harbaugh and others, 2000). Spring discharges were simulated as drains in layer 4 (table 3). The major surface-water features: Colorado River, Death Valley, Great Salt Lake, Humboldt River, Lake Mead, Sevier Lake, Sevier River, Virgin River, and Utah Lake were simulated as general-head boundaries that were specified in layer 3 (fig. 13).

Groundwater pumping is not simulated in the GBNP-C model because steady-state conditions prior to development were simulated. Groundwater currently is pumped from Spring and Snake Valleys for irrigation and totaled 50,000 acre-ft/yr during 2005 (Welch and others, 2007). Irrigation pumping was simulated in the transient, predictive model.
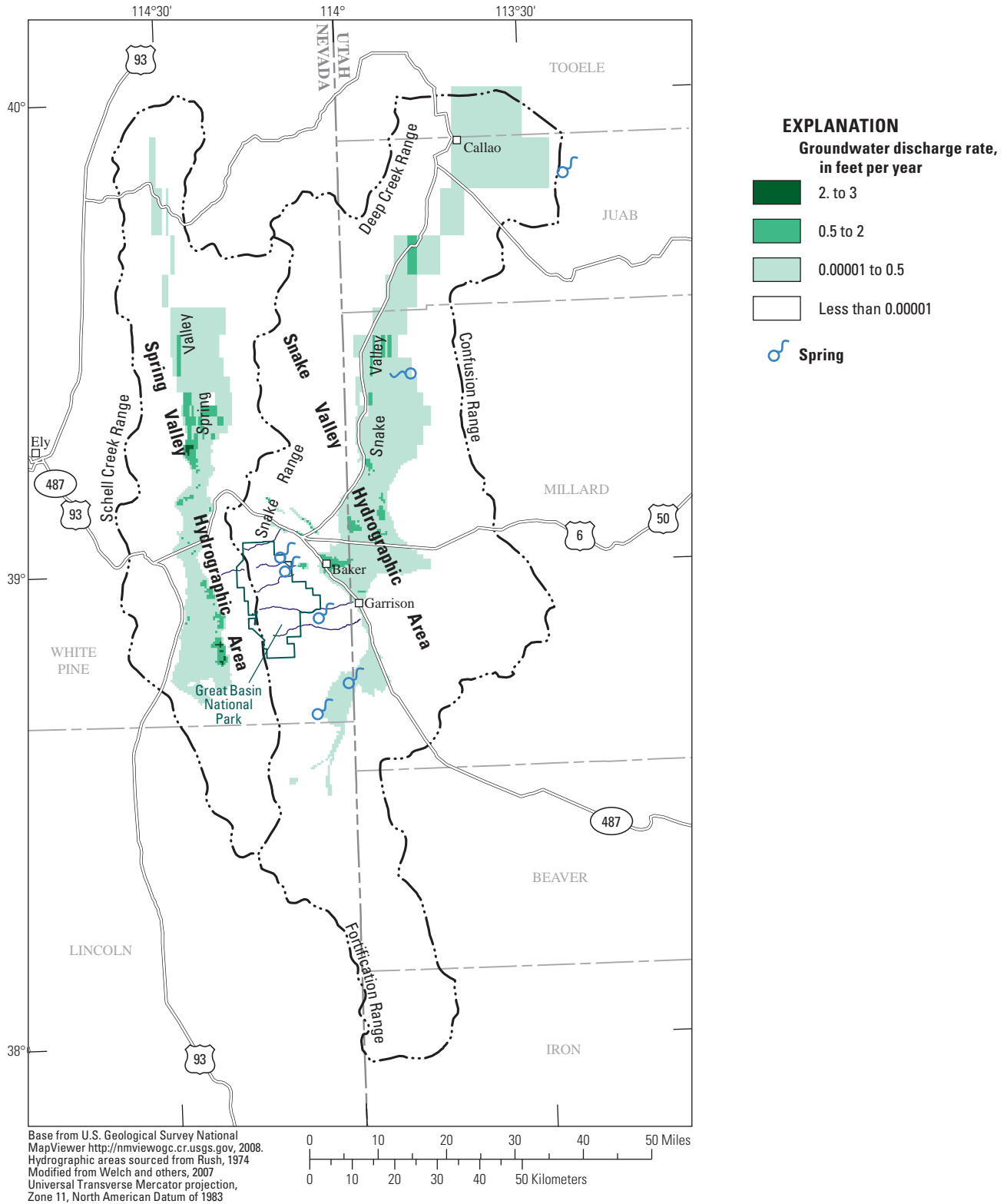
Figure 12. Groundwater discharge from phreatophytes and springs in the GBNP-C model, Spring and Snake Valley, Nevada and Utah.

Table 3.   Stage and simulated discharges from springs in the GBNP-C and RASA models.

[Stage is the minimum pool elevation in feet above North American Vertical Datum of 1988 (NAVD 88). na, not applicable]

Spring or gaining reach	Layer in GBNP–C model	Stage	Simulated spring discharge, in acre-feet per year	
			GBNP–C model	RASA model
Inside Spring and Snake Valleys				
Big Springs	3	5,570	7,000	na
Big Springs run near NV-UT boundary	3	5,446	8,300	na
Cave Spring	2	7,200	100	na
Home Farm Springs	3	5,915	900	na
Kious Spring	3	6,006	400	na
Lehman Creek	1	6,080	2,200	na
Rowland Spring	2	6,580	700	na
Spring Creek Spring	4	6,120	1,400	na
Strawberry Creek	1	6,640	200	na
Twin Springs	4	4,810	4,000	4,000
Outside Spring and Snake Valleys				
Ash Spring	4	3,610	8,100	11,500
Ash Meadows	4	2,280	12,100	17,000
Blue Lake	4	4,260	17,600	20,100
Campbell Embay.	4	6,100	9,400	7,400
Duckwater	4	5,605	20,000	13,300
Fish Creek	4	6,040	100	2,800
Fish Springs	4	4,300	25,700	25,700
Grapevine Springs	4	2,780	500	700
Hiko and Crystal Springs	4	3,810	13,800	12,400
Hot Creek Springs	4	5,620	0	2,000
Manse Spring	4	2,770	3,000	3,900
Mormon Hot Springs	4	5,290	1,600	2,200
Muddy River	4	1,800	32,000	37,400
Nelson	4	5,900	1,400	1,800
Panaca	4	4,770	8,600	9,900
Railroad Valley	4	4,765	3,100	6,000
Rogers and Blue Point	4	1,580	1,000	1,200
Shipley Spring	4	5,800	3,100	4,400
Warm Springs	4	5,760	3,300	5,000
White River	4	5,220	23,200	23,100
TOTAL			212,800	211,800
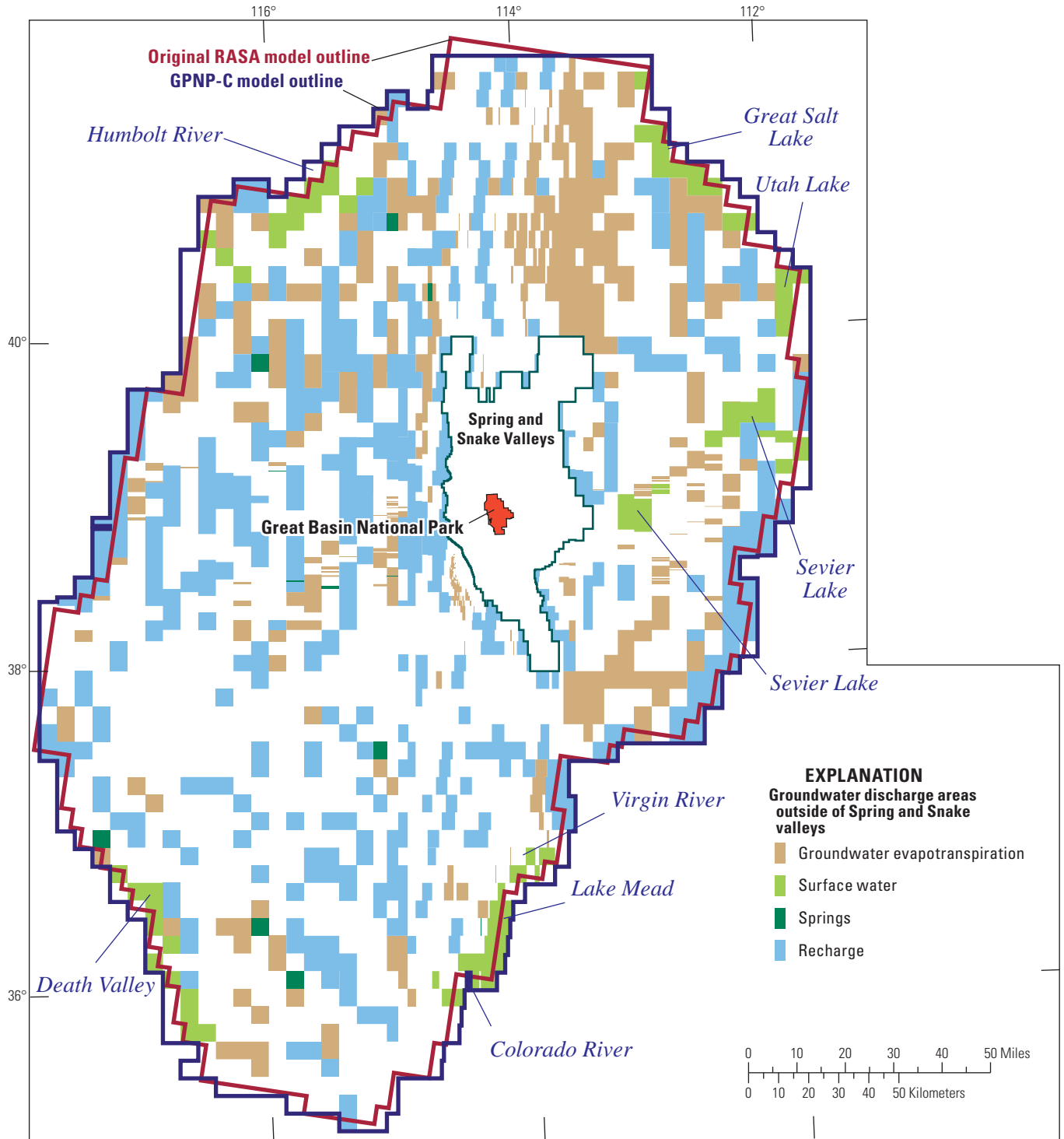
Figure 13.   Groundwater evapotranspiration, surface-water features, and springs in the GBNP-C model that are outside of Spring and Snake Valleys, Nevada and Utah.

Boundary Conditions

The upper boundary of the model was the water table, but transmissivity was not simulated as a function of water-table altitude. Water-table altitudes were known adequately to define typical saturated thicknesses in the basin fill. Steady-state conditions prior to development were simulated so saturated thickness and transmissivity of the basin fill would not change during model calibration. Hydraulic-conductivity estimates compensated for any errors in saturated thickness. These compensating errors were minor given that the uncertainty of hydraulic conductivity is much greater than the uncertainty of the saturated thickness.

The lower model boundary was simulated as a no-flow boundary throughout the study area, which was interpreted as 2,060 ft below the water table in Spring and Snake Valleys. Assigned thicknesses minimally affected results because transmissivities were the primary hydraulic property that was estimated. Minimal groundwater movement was expected at all depths in most mountain blocks because of the occurrence of volcanic, intrusive, and other low-permeability rocks. Deep circulation within the basin fill was not expected because of stratification in the alluvial deposits and increasing cementation with depth. Transmissivity of the basement rocks (layer 4) was estimated directly so assigned thickness did not affect simulated groundwater flow.

Lateral boundaries were simulated as no-flow because model boundaries coincided with surface-water divides or were parallel to directions of groundwater flow (Prudic and others, 1995). These boundaries ranged from 50 to 200 mi from the periphery of Spring and Snake Valleys so the effects of simulated groundwater development in Spring and Snake Valleys likely would not propagate to these boundaries. Surface-water divides occur along ridges of low-permeability mountain blocks and were assumed to be coincident with groundwater divides. Lateral boundary conditions along the periphery of Spring and Snake Valleys were simulated by the supporting RASA model.

Calibration

Recharge, hydraulic-conductivity, and transmissivity distributions of the GBNP-C model were estimated by minimizing a weighted composite, sum-of-squares objective function. About 43 percent of the 813 pilot points that defined these distributions were adjusted with PEST (Doherty, 2008a).

Differences between measured and simulated observations defined the goodness-of-fit or improvement of calibration. These differences, residuals, were weighted and summed in the objective function,

$$\Phi(x) = \sum_{i=1}^{nobs} [(\hat{o}_i - o_i)w_i]^2, \qquad (1)$$

where

x	is the vector of parameters being estimated,
$nobs$	is the number of observations that are compared,
$(\hat{o}_i)$	is the ith simulated observation,
(o_i)	is the ith measurement or regularization observation, and
w_i	is the ith weight. Weights emphasized better measurements and allowed for multiple measurement types that had different units.

Although the sum-of-squares error serves as the objective function, root mean square (RMS) error was reported because RMS error was compared easily to measurements. Root mean square error is,

$$RMS = \sqrt{\Phi / \sum_{i=1}^{nobs} w_i^2}, \qquad (2)$$

Measurement and regularization observations controlled model calibration. Measured water levels, simulated water levels from original RASA model, depth-to-water beneath groundwater evapotranspiration area, spring discharges, land-surface altitudes, spring discharge at Fish Springs, and changes in discharge on selected creek reaches were measurement observations. Estimated values are guided by regularization observations to preferred conditions where parameters are insensitive to measurement observations. This approach is Tikhonov regularization (Doherty, 2008a).

Tikhonov regularization limited recharge, hydraulic conductivity, and transmissivity estimates at pilot points to reasonable values (Doherty, 2003). Sharp differences between nearby values in similar hydrogeologic units were penalized to ensure relatively continuous recharge, hydraulic conductivity, and transmissivity distributions. Unrealistic hydraulic property distributions were avoided by limiting the fit between measured and simulated observations (Fienen and others, 2009). This irreducible, weighted-measurement error combined measurement and numerical model errors.

Measurement Observations

Measured and simulated water levels were compared from 140 wells in Spring and Snake Valleys (fig. 14). More than 85 percent of the wells were screened in basin fill and the remaining 20 wells were completed in carbonate rock (appendix A). Simulated water levels were linearly interpolated laterally to points of measurement from the centers of surrounding cells but were not interpolated vertically (Doherty, 2008b). Measured water levels were weighted more than other observation types because these were the least ambiguous measurement observations.

Continuity with the remainder of the RASA model area was tested with 188 additional water levels that surrounded Spring and Snake Valleys. These water levels were simulated with the original RASA model (Prudic and others, 1995) at 94 mapped locations in layers 3 and 4 (fig. 14). The water levels sampled from the original RASA model became measurement observations for the GBNP-C model.

Depth-to-water beneath GW_{ET} and land-surface altitude observations were defined with a Digital-Elevation Model (DEM) that sampled 1:24,000-scale maps every 30 m and reported to the nearest whole meter (U. S. Geological Survey, 1999). At least 256 points from the DEM were in the smallest model cells. The range of DEM altitudes in the smallest cells typically was from less than 10 ft on the valley floors to more than 1,100 ft in the Snake Range. Observations of depth-to-water beneath GW_{ET} were land-surface altitude minus 5 ft and occurred at every GW_{ET} cell, which created 5,037 observations (fig. 14). Land-surface altitude observations were sampled at 7,601 locations. Each simulated water level that was below land surface was replaced with the land-surface altitude so the residual equaled zero and did not affect model calibration. For example, a simulated water table of 6,500 ft would be changed to 7,000 ft where land-surface altitude is 7,000 ft and the residual would be 0 ft. A simulated water table of 7,500 ft at the same location would not be changed and the residual would be 500 ft.

The supporting spring stage was an observation at most springs because spring discharges were specified (table 3). Supporting spring stage was the pool elevation plus 10 ft. Fish Springs was an exception because the spring was outside of Spring and Snake Valley. Fish Springs was simulated as a drain, as in the original RASA model (Prudic and others, 1995). Simulated discharge was compared to measured discharge from Fish Springs in the objective function.

Losses from Baker Creek and gains on Lehman Creek were simulated with specified heads in the GBNP-C model because creek stages were known better than the distribution of gains and losses. Baker Creek loses 2,900 acre-ft/yr (4 ft^3/s) and Lehman Creek gains 2,200 acre-ft/yr (3 ft^3/s) along the reaches that bound Lehman Caves and Rowland Spring (Elliott and others, 2006). Simulated losses and gains were compared to measured losses from Baker Creek and gains on Lehman Creek in the objective function.

Weights were adjusted iteratively so all observation types affected model calibration. Measured water levels, water levels that were simulated with the original RASA model, depth-to-water beneath GW_{ET}, land-surface altitude, and supporting spring-stage observations were assigned weights of 1, 0.1, 0.2, 0.3, and 1, respectively. Water levels that were simulated with the original RASA model were assigned the smallest weights because these observations exist where hydraulic properties are not changed by calibration. Discharge from Fish Springs, losses from Baker Creek, and gains on Lehman Creek were weighted differently because of unit differences between discharges and water levels.

Observation weights were not assigned to reflect measurement error because model-discretization error typically dominates measurement error (Belcher, 2004). Model-discretization errors have been assigned previously with a contrived equation (Faunt and others, 2004; eq. 2, p. 281). This approach seems like a fool's errand because the equation appears to have been created around the irreducible error of a calibrated model. Absolute values of weights did not affect calibration results because model fit was evaluated exclusively with unweighted residuals.

Regularization Observations

Regularization observations were equations that defined preferred relations between pilot points that defined recharge, hydraulic-conductivity, or transmissivity distributions. Regularization observations affected calibration most where the GBNP-C model was insensitive to measurement observations. Homogeneity was the primary relation that was enforced with Tikhonov regularization (Doherty and Johnston, 2003). Regularization observations that related pilot points within 20 mi of one another were weighted equally. Inverse-distance weighting was used where pilot points were separated by more than 20 mi.

Ratios of initial estimates of recharge rates were the preferred relation between pilot points for the recharge distribution. Initial recharge estimates were assigned to pilot points by precipitation accumulation zone (fig. 11). Preferred relations were defined between pilot points with the same simplified surface geology (fig. 9). For example, a regularization observation was created where two pilot points were in coarse-grained basin fill; but a regularization observation was not created where one point was in coarse-grained basin fill and the other point was in carbonate rock. More than 5,400 regularization observations constrained recharge estimates with these preferred relations.

EXPLANATION

Observation location and type

- • Well with measured water level
- ◇ Simulated water level from RASA model
- ○ Depth to water beneath groundwater evapotranspiration area
- + Land-surface altitude
- ⌀ **Spring**

Base from U.S. Geological Survey National
MapViewer http://nmviewogc.cr.usgs.gov, 2008.
Hydrographic areas sourced from Rush, 1974
Modified from Welch and others, 2007
Universal Transverse Mercator projection,
Zone 11, North American Datum of 1983

Figure 14. Locations of measured water levels, simulated water levels from original RASA model, groundwater evapotranspiration discharge areas, springs, and land-surface altitudes observations in the GBNP-C model.

Homogeneity within simplified geologic classes was the preferred relation between pilot points for the hydraulic conductivity and transmissivity distributions. Hydrogeologic classes were incorporated as observations, instead of as parameters, so hydraulic conductivity or transmissivity in a hydrogeologic class could differ where dictated by measurement observations. Volcanic, intrusive, and other low-permeability units were assumed to have uniformly low hydraulic conductivities, which were reflected in the regularization observations. A preferred heterogeneity was specified where coarse-grained basin fill was assumed to be 30 times more permeable than fine-grained basin fill. More than 5,800 regularization observations constrained hydraulic conductivity and transmissivity estimates with these preferred relations.

Goodness of Fit and GBNP-C Model Results

Simulation results and observations compared favorably in the vicinity of Spring and Snake Valleys where water levels and discharges were compared. Average and RMS water-level errors of 10 and 39 ft, respectively, were not great relative to the 5,400 ft range of measured water levels (fig. 15). Measured water levels ranged from 4,340 to 10,630 ft above NAVD 88 near Callao, Utah, and Baker Lake, Nevada, respectively. The range of measured water levels was similar to simulated water levels that ranged from 4,360 to 10,620 ft above NAVD 88. Minimum and maximum water-level errors ranged from -156 to 128 ft and occurred in northern Snake Valley where the GBNP-C model is discretized coarsely. About 85 percent of simulated water levels were within 50 ft of measured water levels.

An error of 775,000 ft² or an RMS error of about 40 ft was estimated to be the irreducible, weighted-measurement error. Model error could be estimated only from model calibration because numerical model errors typically exceed measurement errors (Belcher, 2004). Model error asymptotically approached the estimated error of 775,000 ft², which could have been any value between 750,000 and 800,000 ft².

Measured water levels, residuals, and simulated water-level contours are mapped for each layer in Spring and Snake Valleys and in the area of interest in appendix B. Measured water levels and residuals are posted on separate maps with simulated water-level contours for each layer. Simulated water levels from GBNP-C model, measured water levels, simulated water levels from original RASA model, depth-to-water beneath GW_{ET}, land-surface altitude, and spring-stage observations are reported in an interactive Microsoft© Excel workbook in appendix C.

Water-level residuals with absolute values greater than 50 ft were considered significant. About 80 percent of the simulated water levels and depth-to-water beneath GW_{ET} residuals are within 50 ft of measured targets because RMS errors are 39 and 41 ft, respectively. Water-level residuals of less than 50 ft also are small relative to the more than 2,000 ft range of water levels in the basin fill in Spring and Snake Valleys (fig. 16). Locations, simulated values, measured values, and residuals are reported for all observations in appendix C.

Water-level residuals exhibited little spatial pattern in the basin fill except surrounding Spring and Snake Valleys where hydraulic properties from the original RASA model were specified (fig. 16). Residuals were greatest where low-permeability intrusive and volcanic rocks were simulated more accurately in Spring and Snake Valleys. Areas west of Spring Valley and surrounding southern Snake Valley were affected by a strong transmissivity contrast. The transmissivity distribution from the original RASA model was more generalized, whereas the transmissivity distribution that was estimated with the GBNP-C model was more representative of the mapped hydrogeologic units (fig. 9).

The distribution of significant water-level residuals and altitudes in the basement rock (model layer 4) were similar to those in the basin fill (fig. 17). Significant residuals in the basement rock primarily occurred outside of Spring and Snake Valleys in the same areas where significant residuals occurred in the overlying basin fill. Simulated water-level differences between basin-fill and carbonate-rock aquifers typically were less than 10 ft in Spring and Snake Valleys.

Transmissive structures were estimated consistently even though hydraulic property estimates at pilot points were non-unique. Areas of transmissivity in excess of 10,000 ft²/d occurred along eastern Snake Valley (fig. 17) and south of the Snake Range in Spring and Snake Valleys (fig. 16). These relatively high-transmissivity structures persisted during all phases of model calibration. Simulated water levels were affected and flow was deflected from the east to the north by these structures.

Hydraulic-property distribution and pilot-point estimates are mapped for all layers in Spring and Snake Valleys and in the area of interest in appendix B. Distributions and pilot-point estimates of hydraulic conductivity are mapped for layers 1, 2, and 3. The distribution and pilot-point estimates of transmissivity are mapped for layer 4. The transmissivity of all four layers also is reported in appendix B. Pilot-point locations, interpreted geology, simulated thickness, and parameter estimates are reported in appendix D.
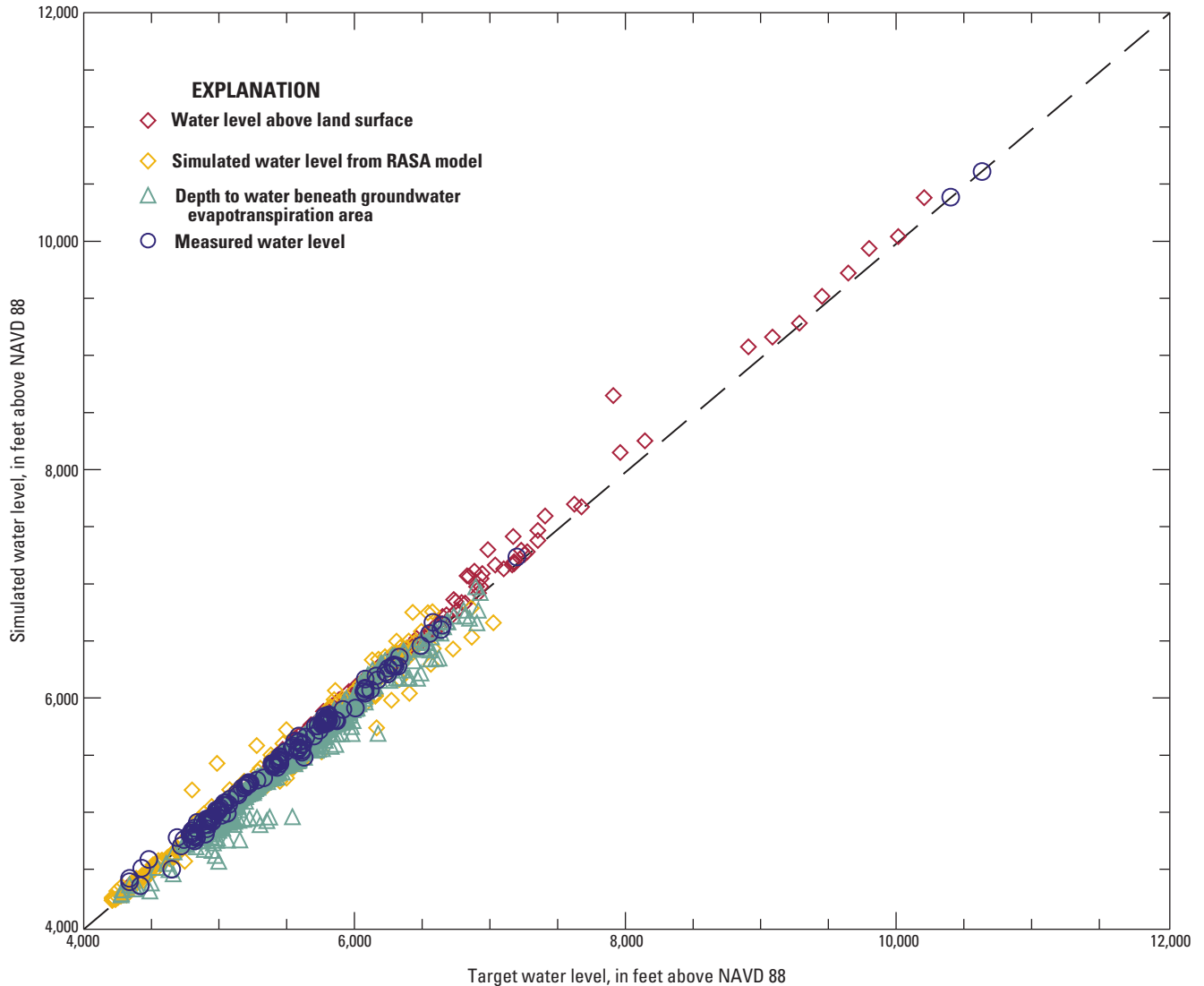
Figure 15.   Simulated and target water levels for the calibrated GBNP-C model, Nevada and Utah.

Recharge was generated principally by the Snake Range and the Schell Creek Range to a lesser degree (fig. 18). The estimated distribution of recharge was similar to the potential recharge distribution (fig. 11). Maximum annual recharge rates were about 10 ft and occurred as mountain-front recharge just downgradient from the contact between basement rocks and basin fill. The annual volume of recharge to Spring and Snake Valleys consistently was estimated around 260,000 acre-ft. The simulated recharge distribution and pilot-point estimates are mapped in Spring and Snake Valleys and in the area of interest in appendix B. Pilot point locations, interpreted geology, and recharge rate estimates are reported in appendix D.

The GBNP-C model simulated more groundwater flow through Spring and Snake Valleys than the original RASA model (table 4). This largely occurred because annual simulated GW_{ET} and spring discharge from Spring and Snake Valleys in the GNBP-C model was 64,000 acre-ft greater than from the original RASA model. The GNBP-C model also simulated local flow in the mountain blocks that was not simulated by the original RASA model. Recharge to the GNBP-C model in Spring and Snake Valleys included the net, annual addition of 23,000 acre-ft from specified heads in the mountain blocks. Simulated water budgets in the study area outside of Spring and Snake Valleys were similar in both the GNBP-C and original RASA models (table 4).

Figure 16. Estimated transmissivities, simulated water-level contours, and water-level residuals in the basin fill in model layer 3, Nevada and Utah.

Figure 17. Estimated transmissivity, simulated water-level contours, and water-level residuals in the basement rocks in model layer 4, Spring and Snake Valleys, Nevada and Utah.

Figure 18.   Calibrated recharge distribution and pilot points for GBNP-C model in Spring and Snake Valleys, Nevada and Utah.

Table 4.   Water budgets simulated with the GBNP-C and original RASA models, Spring and Snake Valleys, Nevada and Utah.
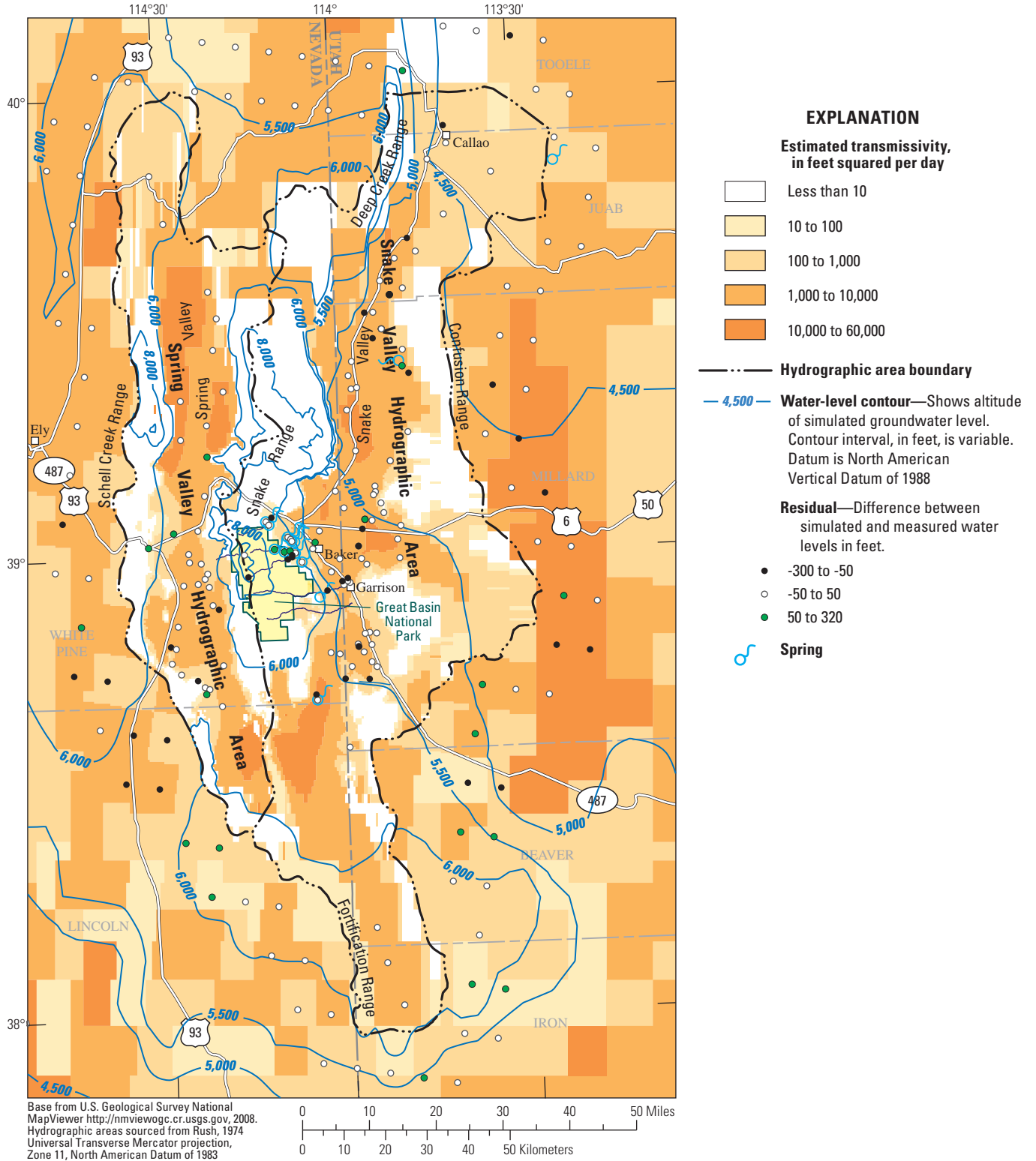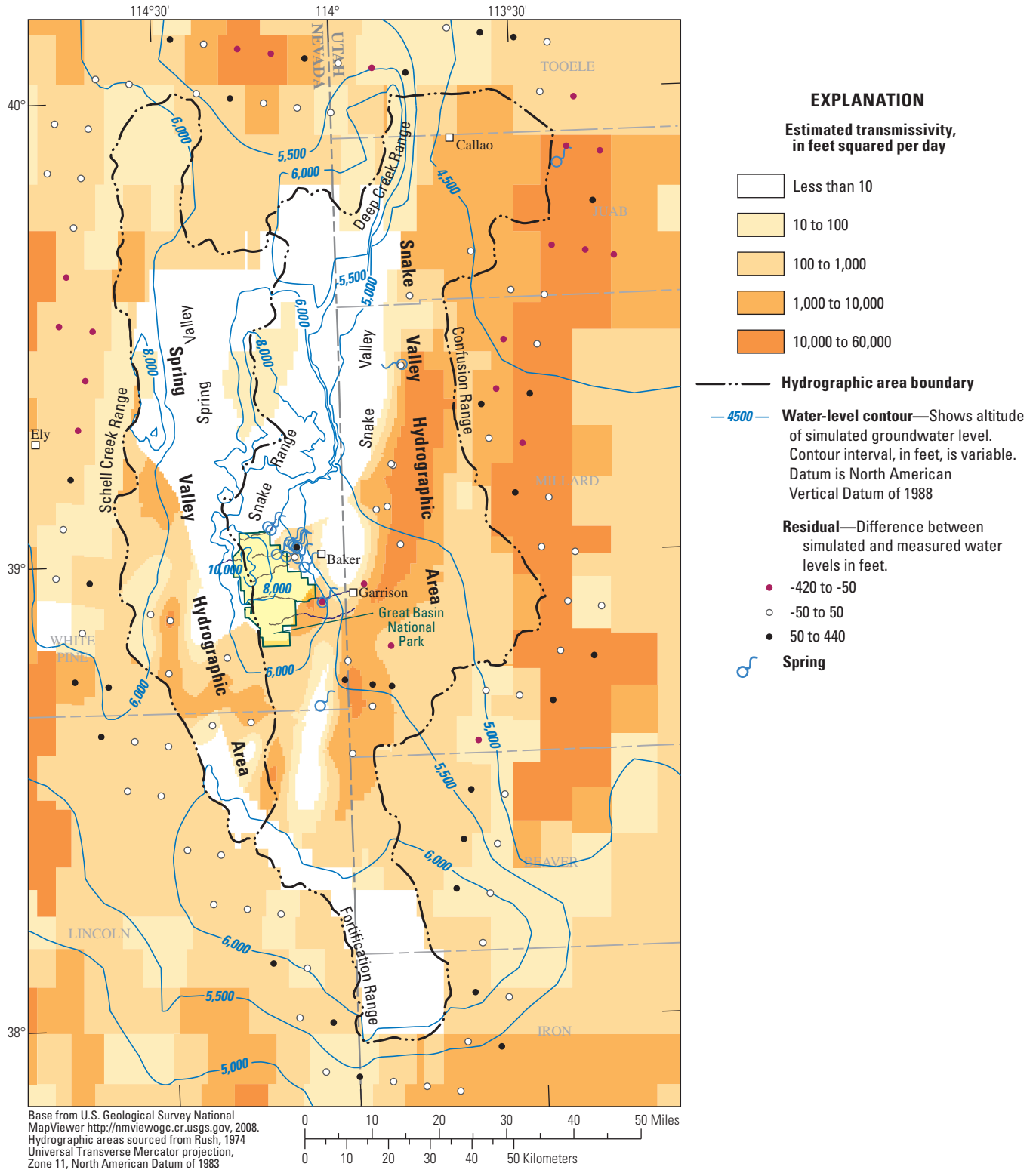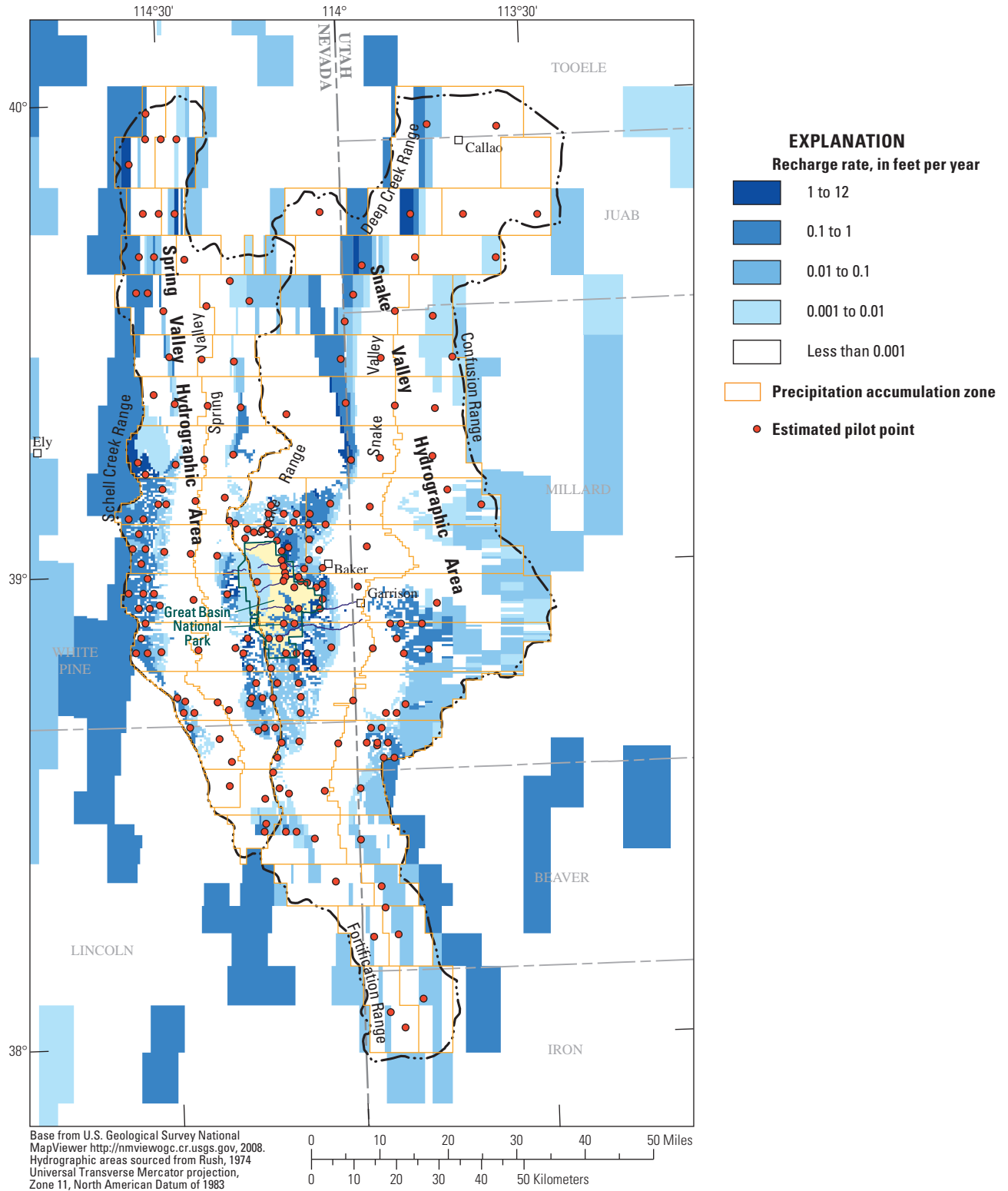
[All values are in thousands of acre-feet per year. Values may not match presented values due to rounding. **GBNP-C** is the Great Basin National Park calibration model. **RASA** is the original Great Basin Regional Aquifer System Analysis model (Prudic and others, 1995)]

Budget component	Study area outside of Spring and Snake Valleys		Spring and Snake Valleys	
	GBNP-C	**RASA**	**GBNP-C**	**RASA**
INFLOW				
Recharge[1]	1,342	1,341	259	183
Spring and Snake Valleys	49	37	–	–
Total inflow	1,391	1,378	259	183
OUTFLOW				
GW_{ET}[2]	1,084	1,071	187	142
Spring discharge	188	208	23	4
Surface water	104	99	0	0
Spring and Snake Valleys	–	–	49	37
Total outflow	1,376	1,378	259	183

[1]Recharge is the sum of recharge and flow to specified heads in mountain blocks in Spring and Snake Valleys.

[2]GW_{ET} is groundwater discharge by evapotranspiration in excess of local precipitation.

Alternative Models

Transmissivity estimates were affected primarily by the magnitude and distribution of groundwater-discharge estimates. About 90 percent of the 210,000 acre-ft of annual discharge from Spring and Snake Valleys was simulated as distributed GW_{ET} in the GBNP-C model (table 4). These discharge rates are uncertain, but were assumed as known while calibrating the GBNP-C model.

A significant uncertainty is associated with the distributed GW_{ET} estimates from Spring and Snake Valleys because the average groundwater-discharge rate of 0.2 ft/yr is small relative to the measured quantities (Moreo and others, 2007). Groundwater-discharge rates were the differences between measured evapotranspiration and precipitation rates, which averaged 0.6 and 0.4 ft/yr, respectively. An uncertainty of ±0.05 ft/yr could be expected in the groundwater-discharge rates, which would cause annual distributed GW_{ET} from Spring and Snake Valleys to range from 151,000 to 227,000 acre-ft (table 5).

The uncertainty in distributed groundwater-discharge rate of ±0.05 ft/yr was a maximum tolerable value. Tolerance was defined by annual distributed GW_{ET} discharges of 122,000 and 151,000 acre-ft from Spring and Snake Valleys for decreases in distributed groundwater-discharge rates of 0.10 and 0.05 ft/yr, respectively. A 20 percent decrease in diffuse groundwater-discharge estimates was tolerable but a 40 percent decrease was not. This was because the mapped vegetation distribution and associated groundwater discharge would differ visibly in response to existing pumping for irrigation in Snake Valley.

The effects of uncertain distributed GW_{ET} estimates on transmissivity estimates were bounded with alternative models, GBNP-LowET and GBNP-HighET, that were calibrated to the lower and upper rates of

distributed GW_{ET}, respectively. The alternative models were calibrated to the objective function that was defined for the GBNP-C model. Recharge, hydraulic conductivity, and transmissivity at the same pilot points defined in the GBNP-C model were estimated to calibrate the alternative models. Recharge, hydraulic-conductivity, and transmissivity estimates that calibrated the GBNP-C model became the initial parameter estimates for the alternative models. All three models equally fit the observations with weighted-measurement errors between 780,000 and 790,000 ft^2 or RMS errors of about 40 ft.

All recharge changed about 10 percent more than changes in distributed GW_{ET} in Spring and Snake Valleys (table 5). Recharge and induced flow from specified heads increased 45,000 acre-ft/yr in the GBNP-HighET model, while distributed GW_{ET} increased 40,000 acre-ft/yr. Proportionate reductions also occurred in the GBNP-LowET model. Disproportionate changes in recharge and discharge were balanced by changes in subsurface flow between Spring and Snake Valleys and the remainder of the study area.

About 75 percent of the annual recharge volume entered Spring and Snake Valleys at rates between 0.2 and 4 ft for the GBNP-C and alternative models (fig. 19). The annual recharge volume consistently totaled 30,000 acre-ft from areas with annual recharge rates less than 0.2 ft in all three models.

Transmissivity of all model layers differed by less than a factor of 2 between the GBNP-HighET and GBNP-LowET models through more than 96 percent of Spring and Snake Valleys (fig. 20). Transmissivity of the basin fill increased between the Snake Range and the groundwater-discharge areas and through the playas in northern Snake Valley. The transmissivity of the carbonate rock through the Confusion Range in eastern Snake Valley decreased as recharge increased.

Transmissivity estimates were minimally sensitive to groundwater-discharge estimates east of GBNP (fig. 20). Transmissivity estimates in the basin fill between Baker and Big Springs changed less than 50 percent between the two alternative models. This indicates that drawdown from proposed groundwater development in Snake Valley can be estimated with transmissivity distributions from the GBNP-HighET, GBNP-C, and GBNP-LowET models and the results will differ little.

Table 5.   Water budgets simulated with GBNP-C, GBNP-LowET, and GBNP-HighET models in Spring and Snake Valleys, Nevada and Utah.

[All values are in thousands of acre-feet per year. Values may not match presented values due to rounding. **GBNP-C** is the Great Basin National Park calibration model. **GBNPLowET** is the alternative Great-Basin National Park model, where annual GW_{ET} has been reduced by 0.05 foot. **GBNP-HighET** is the alternative Great-Basin National Park model, where annual GW_{ET} has been increased by 0.05 foot]

Budget component	Spring and Snake Valleys		
	GBNP-C	GBNP-LowET	GBNP-HighET
INFLOW			
Recharge	234	199	276
Specified heads in mountain blocks	36	34	39
Spring and Snake Valleys	19	18	21
Total inflow	289	251	336
OUTFLOW			
GW_{ET}[1]	187	151	227
Specified heads in mountain blocks	12	11	12
Spring discharge	23	23	23
Spring and Snake Valleys	68	66	74
Total outflow	289	251	336

[1]GW_{ET} is groundwater discharge by evapotranspiration in excess of local precipitation.
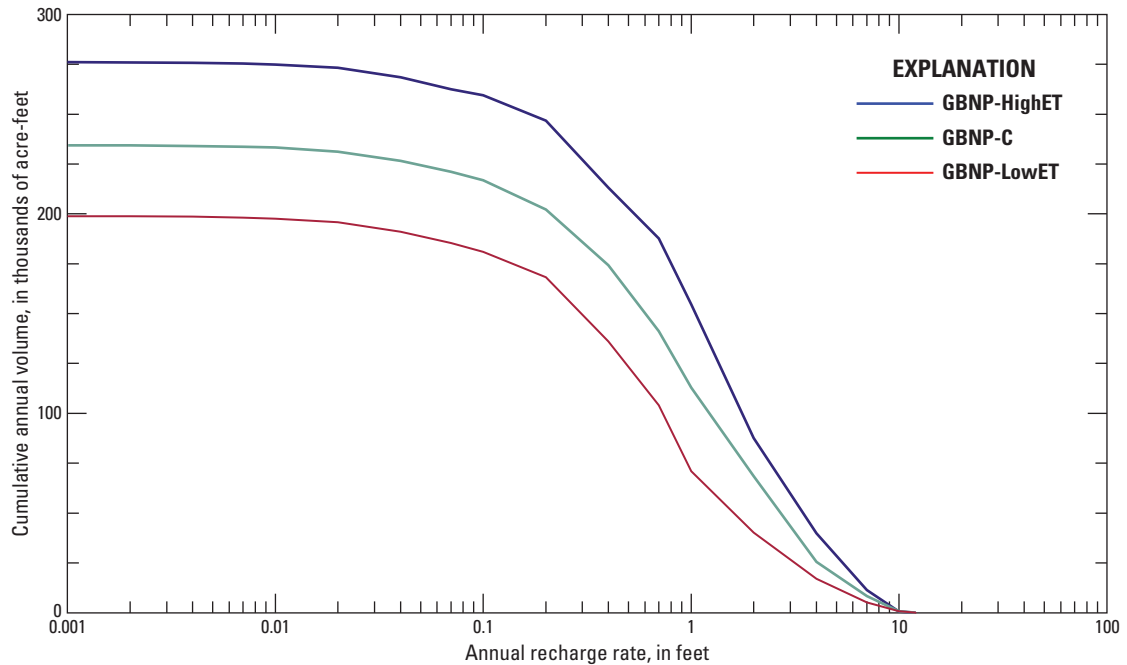

Figure 19.   Cumulative recharge volumes for GBNP-HighET, GBNP-C, and GBNP-LowET models, Spring and Snake Valleys, Nevada and Utah.
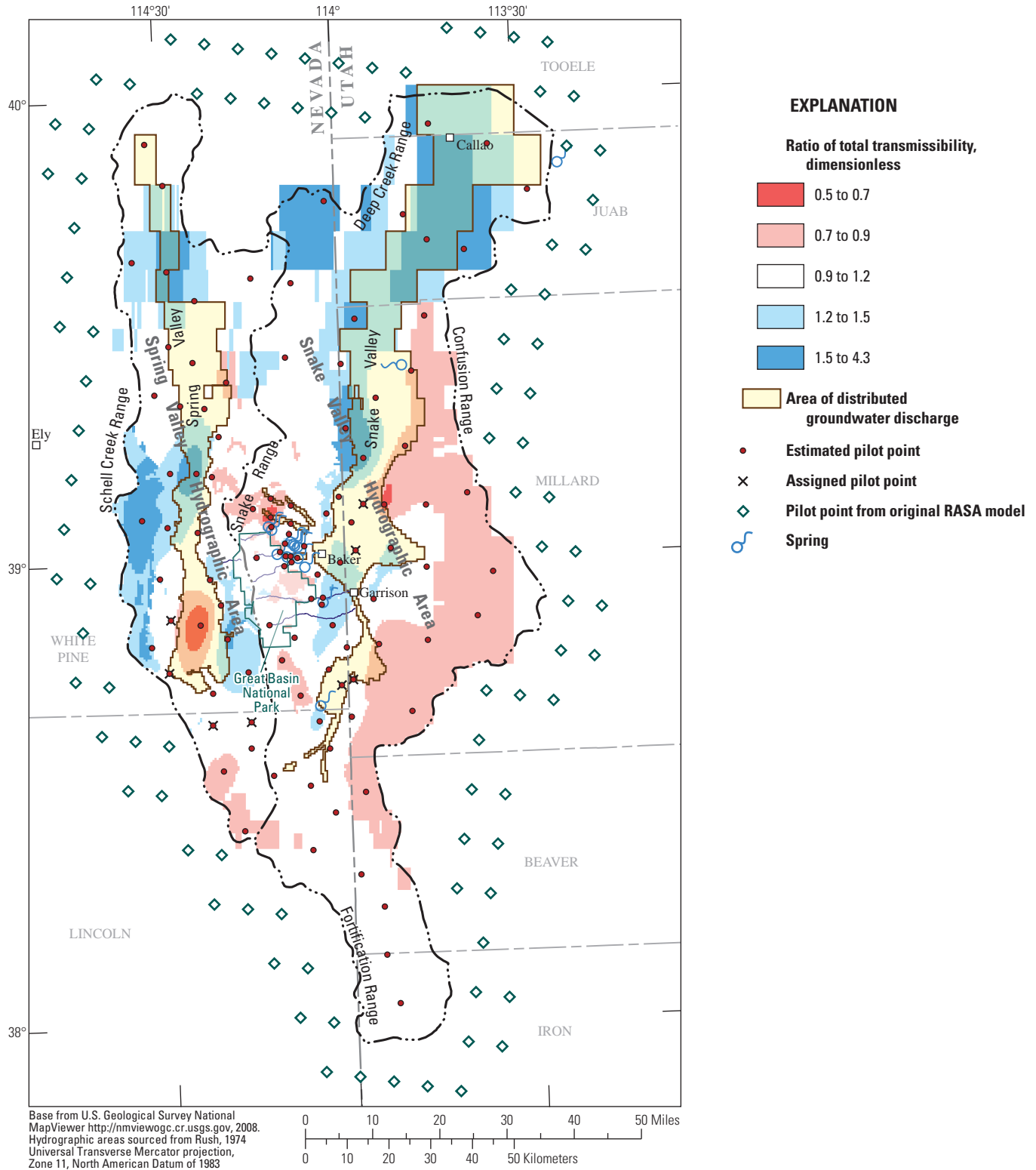
Figure 20.   Ratio of GBNP-HighET transmissivity divided GBNP-LowET transmissivity (layers 1–4), Spring and Snake Valleys, Nevada and Utah.

Potential Effects of Groundwater Pumping from Snake Valley

The Great Basin National Park predictive (GBNP-P) model was developed to estimate the potential effects of pumping from Snake Valley on springs, streams, and water levels in caves in and adjacent to GBNP (fig. 1). Pumping from Snake Valley includes existing withdrawals for irrigation and proposed groundwater development. The GBNP-P model was a transient groundwater-flow model where changes in groundwater storage were simulated. The hydraulic conductivity of basin fill and transmissivity of basement rock were the same distributions that were estimated with the GBNP-C model. Specific yield was estimated from aquifer tests in Spring and Snake Valleys (table 1) and distributed with the surface geology (fig. 9).

Pumped groundwater comes from storage and reductions in discharge to streams, springs, wetlands, and phreatophytes. Groundwater storage, which is derived from the compressibility of the aquifer system under confined conditions and gravity drainage of pores under unconfined conditions (at the water table), is the initial source of water to new pumping wells (Bredehoeft and Durbin, 2009). Groundwater discharge to streams, springs, wetlands, and phreatophytes is the ultimate source of pumped groundwater after a new equilibrium (no change in storage) is reached. This source will be referred to as groundwater capture.

Hydraulic diffusivity largely controls the delay between the start of pumping and most water being supplied by groundwater capture. Hydraulic diffusivity is the ratio of transmissivity divided by storage coefficient. Characterizing pumping responses with hydraulic diffusivity implies that an aquifer system is two-dimensional and vertical differences in drawdown are minor. This simplification is reasonable when analyzing drawdowns and groundwater capture that occur during decades of groundwater development. Simplifying multiple, three-dimensional, hydraulic-property distributions to a single hydraulic-diffusivity distribution helps assess the sensitivity of GBNP-P model results to errors in hydraulic-property estimates.

Direct-Drawdown Approach

Direct simulation of drawdown reduced model complexity and uncertainty because fewer hydrologic features were simulated. Model input, other than the proposed pumpage, was limited to hydraulic-conductivity, transmissivity, storage-coefficient, and groundwater-discharge distributions (Leake and others, 2010). The drawdown models simulated changes so relatively unchanging quantities, such as recharge and existing pumpage distributions, do not need to be simulated explicitly. The absence of these features simplified presentation of model results and avoided the uncertainty associated with recharge and historic pumping estimates.

Simulation of groundwater capture will better conform to a mapped distribution with the direct-drawdown approach than with extrapolation of a calibrated model. Groundwater discharge that is simulated with a calibrated model will spatially deviate from the mapped groundwater discharge, even where total simulated and measured discharges are equal. The availability of groundwater discharge that can be captured is defined directly from mapped discharges with the direct-drawdown approach, so simulated capture cannot exceed measured discharge at each cell.

The availability of groundwater discharge that can be captured in Spring and Snake Valleys is limited. Simulated groundwater capture from springs cannot exceed measured discharges, which range between 100 and 8,300 acre-ft/yr in Snake Valley (table 3). Simulated groundwater capture from phreatophytes and wetlands, which is distributed areally, is limited to rates that average 0.2 ft/yr and do not exceed 3 ft/yr (Welch and others, 2007).

Groundwater capture that is limited by availability can be simulated accurately with wells and drains in MODFLOW (Harbaugh and others, 2000). Observed discharge rates are injected into the model with wells, Q_{WEL}, and removed with drains, Q_{DRN} (fig. 21). Drain elevations are the extinction depths below the existing water table. Drain conductances are the observed discharge rates divided by the extinction depths. Differences between injected and drained water, simulate the reduction in groundwater discharge that pumping captures. The direct-drawdown approach limits the amount of captured groundwater to measured discharges. Variations of this approach have been applied in finite-element models (Durbin and others, 2008). Combining existing packages to simulate a function not supported formally in MODFLOW has been applied previously with the river and drain packages (Zaadnoordijk, 2009).

Capture of distributed GW_{ET} and spring discharge were simulated in the GBNP-P model using a combination of well and drain packages in MODFLOW (Harbaugh and others, 2000). Distributed GW_{ET} was captured from layer 1 and could not exceed the mapped GW_{ET} rate (fig. 12). Spring discharges were captured from layers 2, 3, or 4 and could not exceed the measured rates (table 3). A uniform extinction depth of 15 ft was assumed for all distributed GW_{ET} and springs. Uniform extinction depths of 5 ft and 10 ft were tested and minimally changed predicted drawdowns and groundwater capture.

Capture of discharge to streams in low-permeability mountain blocks was simulated with specified heads set to zero. These heads were specified at the bottom of drainages where perennial streams occurred. Groundwater capture was not limited because groundwater/surface-water interaction was minimal and discharge to these streams was less than 5 percent of the volumetric budget in the GBNP-C model (table 5).

Hydraulic conductivity of basin fill and transmissivity of basement-rock distributions from the GBNP-C model were specified in the GBNP-P model (app. B). Transmissivity in the alternative models differed from the GBNP-C model by less than 20 percent in Snake Valley south of Baker (fig. 20).
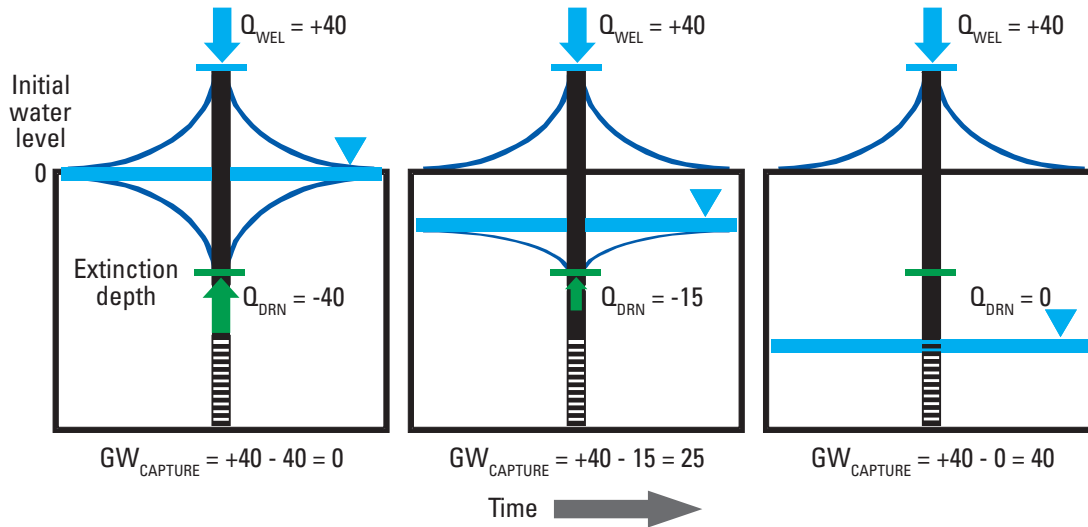
Figure 21.   Example of limited groundwater capture in a cell as simulated in the GBNP-P model with the well and drain packages in MODFLOW where the water table is declining because of regional pumping, Spring and Snake Valleys, Nevada and Utah.

Hydraulic-property distributions from the alternative models were not considered because the range of pumping rates investigated was greater than transmissivity differences between the GBNP-C model and either alternative model (appendix D).

Specific yield was the significant component of storage coefficient in the GBNP-P model because drainage from the water table released 50–100 times more water than aquifer compressibility per foot of drawdown. Specific yields in the basin fill and carbonate rocks were estimated from aquifer tests in Spring and Snake Valleys. Specific yield ranged from 12 to 18 percent in the basin fill and from 1 to 4 percent in the carbonate rocks (table 1). Specific yields of 2 and 15 percent were specified for bedrock and basin fill, respectively, in the GBNP-P model (fig. 9). A uniform specific storage of 2×10^{-6} 1/ft was assigned to layers 2, 3, and 4 in Spring and Snake Valleys and to layer 4 through the remainder of the model.

Reasonable hydraulic-diffusivity estimates in Snake Valley south of U.S. Highway 50 could deviate from the assigned values in the GBNP-P model by as much as 50 percent. This constraint assumes that the average transmissivity could be as much as 20 percent greater than in the GBNP-P model and the specific yield of the basin fill is 12 percent instead of 15 percent. Increasing the hydraulic diffusivity by 50 percent would cause the simulated delay between the start of pumping and detection of drawdown at a site to be 33 percent less (earlier) than in the GBNP-P model. Decreasing the hydraulic diffusivity by 50 percent would cause the simulated delay between the start of pumping and detection of drawdown at a site to be 50 percent greater (later) than in the GBNP-P model.

Estimates of distributed GW_{ET} capture, spring declines, and regional-drawdown extent were affected minimally by not simulating transmissivity as a function of drawdown. This was because the simulated extinction depth for distributed GW_{ET} and spring discharge was 15 ft, which is a minor change relative to saturated thickness of the basin fill. The extent of regional drawdown typically is defined by the 10-foot contour, which also is a slight change relative to saturated thickness of the basin fill. Simulating transmissivity independently of drawdown likely affected model results near proposed points of diversion where simulated drawdowns exceeded 100 ft. Simulated drawdowns of 100 and 200 ft typically would be underestimated by 5 and 13 percent, respectively, in a 1,000-foot thick aquifer because transmissivity was not simulated as a function of drawdown.

Effects of Existing Irrigation

Groundwater withdrawals for irrigation have affected water levels and captured groundwater discharge in Snake Valley. Annual groundwater withdrawals for irrigation in Snake Valley averaged 13,000 acre-ft between 1945 and 2004 (Southern Nevada Water Authority, 2009) and averaged 19,000 acre-ft during 2000, 2002, and 2005 (Welborn and Moreo, 2007). This assumed annual consumptive use for irrigation averaged 2.5 ft. Water levels have declined between 0.3 and 0.7 ft/yr near Baker, Nevada in response to groundwater withdrawals for irrigation since 1990 (U. S. Geological Survey, 2010). The extent and volume of captured groundwater discharge in Snake Valley was estimated with the GBNP-P model.

Potential cumulative effects of irrigation in Snake Valley were simulated by pumping 19,000 acre-ft/yr during a 40-year period. Irrigation pumpage was distributed as observed during 2002 (fig. 22; Welborn and Moreo, 2007) and withdrawn from the basin fill (layer 3). A 40-year period was simulated so the total pumpage (760,000 acre-ft) equaled cumulative pumpage from 1945 to 2004 (Southern Nevada Water Authority, 2009).

Simulated drawdowns of more than 10 ft in the pumping interval (layer 3) extended little beyond the irrigated areas (fig. 22). Simulated drawdowns exceeded 3 ft over 200,000 acres at the end of the 40-year period. Detectable drawdowns occurred primarily in the basin fill except in southern Snake Valley where drawdown from irrigation propagated into the carbonate rocks.

Distributed GW_{ET} primarily was captured at rates of less than 1 ft/yr near the irrigated areas and at rates of less than 0.083 ft/yr more than 2 mi from the irrigated areas (fig. 23). Drawdown propagation at the water table (layer 1) was attenuated where groundwater discharged (fig. 23). Captured groundwater discharge supplied more than 80 percent of 19,000 acre-ft/yr pumped at the end of the 40-year period.

Simulated Drawdown and Groundwater Capture

Total annual potential groundwater withdrawal and the period of analysis were specified by the Nevada State Engineer in section VI of Interim Order no. 2 for the Snake Valley water-rights hearing (Nevada Division of Water Resources, 2008). The order states,

> "The Applicant is hereby ordered to provide a groundwater model that simulates pumping and potential impacts from pumping groundwater in the amount of 10,000 acre-feet annually, 25,000 acre-feet annually, and 50,000 acre-feet annually for the time frames of 10 years, 25 years, 50 years, 100 years, and 200 years."

Potential groundwater-withdrawal locations were limited to nine proposed points of diversion (fig. 24). Each proposed point of diversion was assumed to be a single well that could pump 1,200–3,400 gal/min (2,000–5,600 acre-ft/yr). Wells in more transmissive areas were selected for the 10,000 and 25,000 acre-ft/yr scenarios where only five wells were needed (table 6). All nine wells were pumped to simulate annual pumpage of 50,000 acre-ft/yr from Snake Valley.

Pumpage from the proposed points of diversion was simulated with the multi-node well package (Halford and Hanson, 2002). This approach simulated groundwater pumping from multiple layers, computed drawdown in pumped wells, and limited production rates that exceeded user-specified drawdowns. Screened intervals were assumed to extend from 60 to 2,060 ft below the water table (layers 3 and 4) because depths of withdrawal were unspecified. Diameters of production wells were assumed to be 24 in. A maximum drawdown of 1,000 ft was specified for all wells.

A fourth scenario was simulated where annual pumpage totaled 50,000 acre-ft and drawdown in the production wells was unlimited. This scenario was tested because annual production of 50,000 acre-ft could not be produced when drawdown could not exceed 1,000 ft. Annual production initially totaled 43,000 acre-ft and decreased to 40,000 acre-ft where total withdrawals of 50,000 acre-ft were specified and drawdown was limited. Unlimited production of 50,000 acre-ft/yr was an absurd simulation because drawdown in the well at proposed point of diversion PD-27 exceeded 400,000 ft.

Irrigation pumpage was simulated in addition to potential groundwater pumpage in four additional scenarios because existing irrigation pumping has decreased water levels and captured groundwater discharge. Simulation of potential groundwater pumping is identical to the approach reported for the four previous scenarios (table 6). These four additional scenarios differ because 40 years of pumping 19,000 acre-ft/yr were simulated prior to potential groundwater pumping commencing. Irrigation pumpage was distributed as observed during 2002 (fig. 22; Welborn and Moreo, 2007) and withdrawn from the basin fill (layer 3). Irrigation pumpage of 19,000 acre-ft/yr continued as distributed during the 200-year predictive period.

Results from the eight GBNP-P model scenarios are presented as maps of groundwater capture and drawdown (appendix E), as time series of drawdowns and discharges from selected wells (appendix F), and as time series of discharge reductions from selected springs and volumetric controls (appendix G). Groundwater capture and drawdown maps are presented at the scale of the area of interest and the scale of Spring and Snake Valleys for each layer after 10, 25, 50, 100, and 200 years of pumping for a total of 40 maps per scenario (appendix E). Drawdown and discharge time series from selected wells were simulated with the multi-node well package, including unpumped wells, that were completed in layers 2 and 3 in the mountain block and layers 3 and 4 in the basin fill (appendix F). Simulated discharge reduction is the sum of well and drain packages at selected springs (appendix G, table 3).

Distributed GW_{ET} was captured at a maximum rate of 3 ft/yr and drawdown propagation was attenuated where groundwater discharged at greater rates (fig. 24). Water-table declines propagated farther from pumping wells south of Great Basin National Park because less groundwater discharge was available for capture than near Baker, Nevada. The water table declined minimally north of U.S. Highway 50 because more groundwater discharge was available for capture. General patterns of groundwater capture and water-table declines were similar for all scenarios (appendix E). Simulated drawdowns greater than 1 ft propagate outside of Spring and Snake Valleys after 200 years of pumping (fig. 25). This occurs in all scenarios (appendix E).
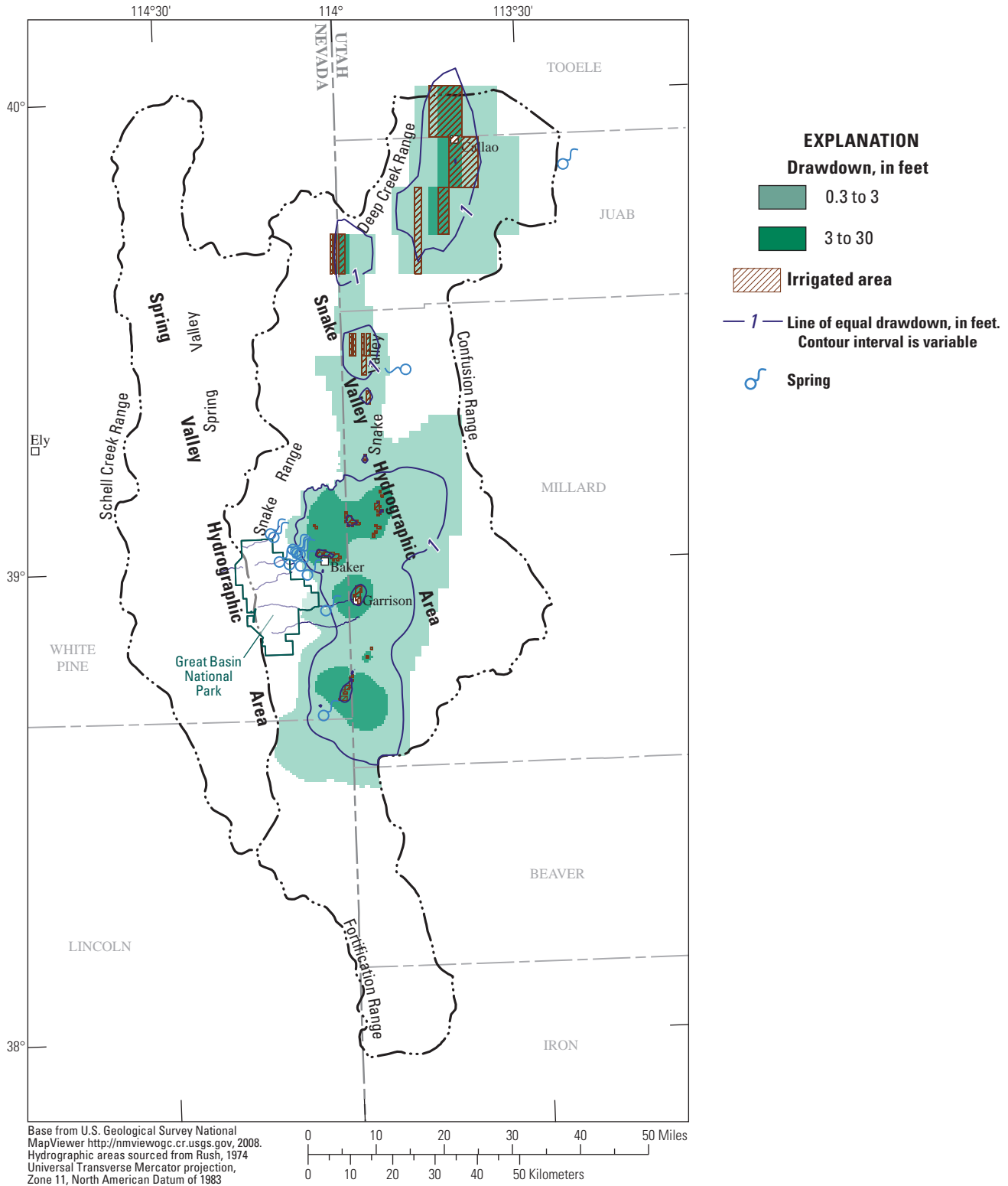
Figure 22.   Irrigated acreage during 2002 and drawdowns in the basin fill (model layer 3) from 40 years of pumping 19,000 acre-ft/yr for irrigation, Snake Valley, Nevada and Utah.
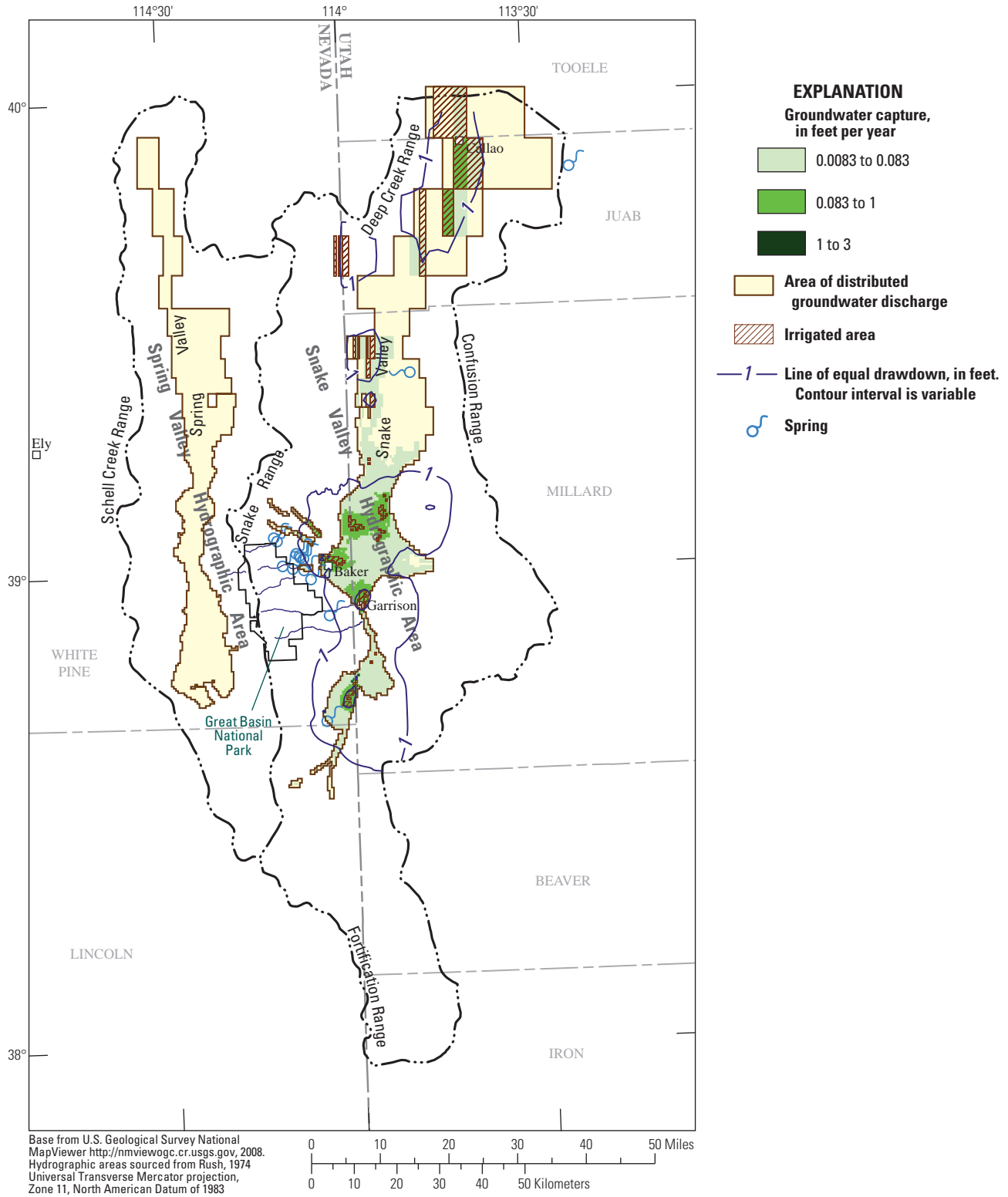
Figure 23. Simulated groundwater capture and drawdown of the water table (model layer 1) from 40 years of pumping 19,000 acre-ft/yr for irrigation, Spring and Snake Valleys, Nevada and Utah.
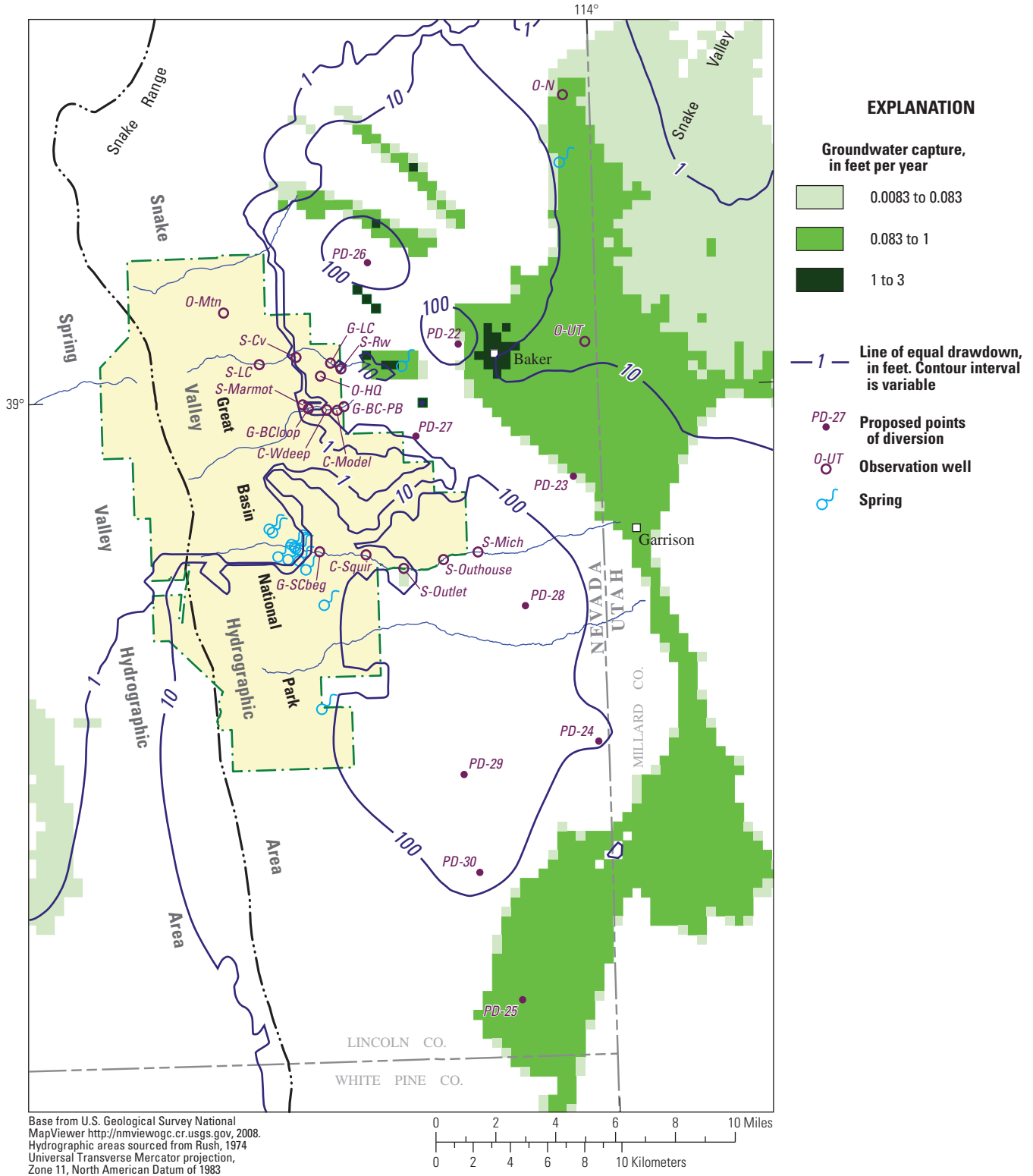
Figure 24. Simulated groundwater capture and drawdown in the area of interest, layer 1 after 200 years of pumping 40,000 acre-ft/yr from Snake Valley, Nevada and Utah.

Figure 25.   Simulated drawdown in Spring and Snake Valleys, model layer 4 after 200 years of pumping 40,000 acre-ft/yr from Snake Valley, Nevada and Utah.

Table 6.   Proposed points of diversion and pumping rates for groundwater development scenarios in southern Snake Valley, Nevada and Utah.

[Easting and Northing are in Universal Transverse Mercator Projection, Zone 11, NAD 83. L suffix in scenario indicates drawdown limited in pumping wells. U suffix in scenario indicates drawdown unlimited in pumping wells. –, well not pumped]

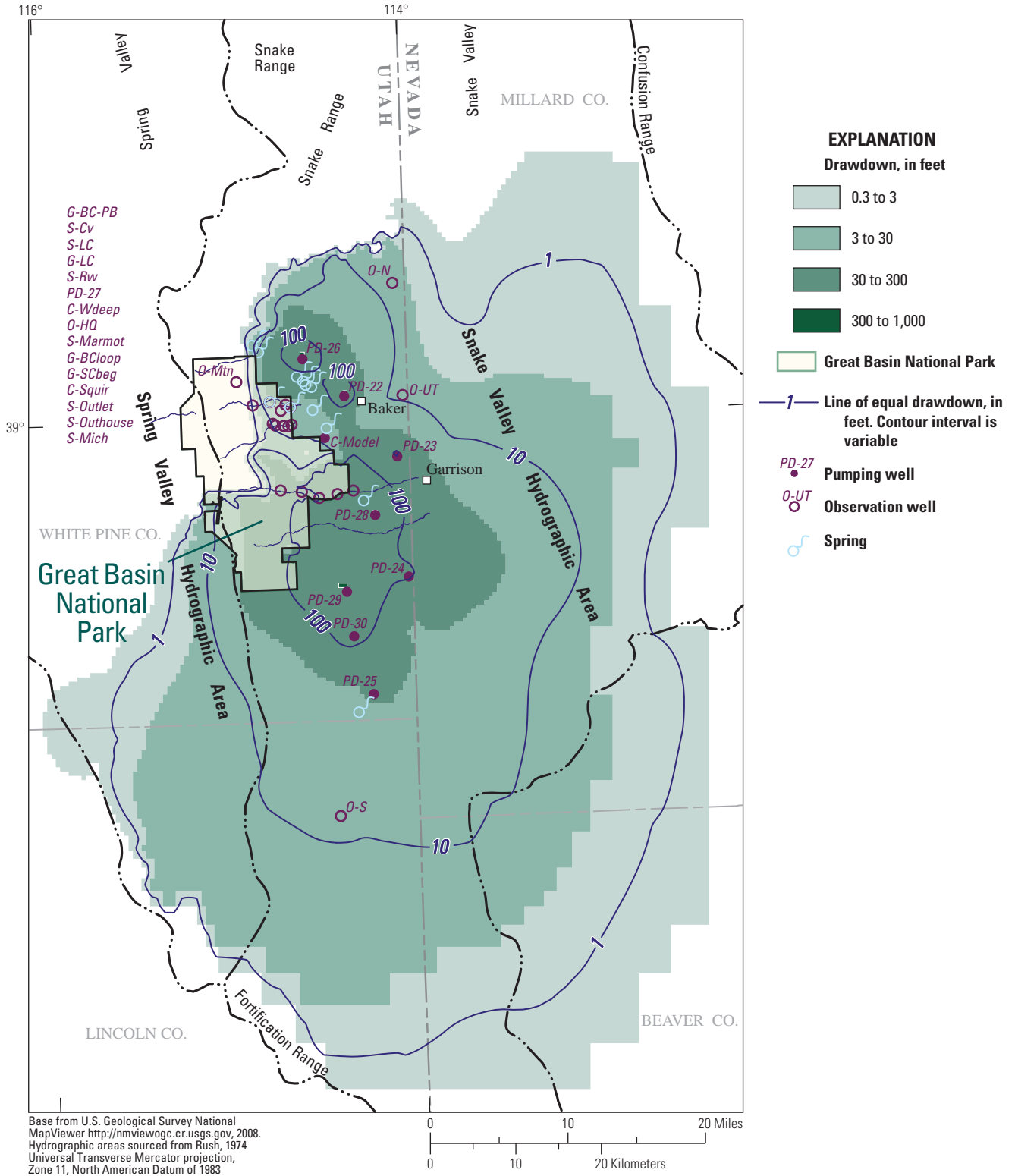| Application Number, Nevada State Engineer	Proposed point of diversion	Easting, m	Northing, m	Groundwater development scenarios			
				Total annual pumpage specified, in acre-feet			
				10,000-L	25,000-L	50,000-L[1]	50,000-U
54022	PD-22	748,062	4,322,770	–	–	5,395	5,556
54023	PD-23	754,254	4,315,753	2,000	5,000	5,556	5,556
54024	PD-24	755,615	4,301,694	2,000	5,000	5,556	5,556
54025	PD-25	751,525	4,287,959	2,000	5,000	5,556	5,556
54026	PD-26	743,191	4,327,091	–	–	3,725	5,556
54027	PD-27	745,799	4,317,881	–	–	12	5,556
54028	PD-28	751,674	4,308,884	2,000	5,000	4,980	5,556
54029	PD-29	748,385	4,299,921	–	–	3,364	5,556
54030	PD-30	749,235	4,294,718	2,000	5,000	5,556	5,556
	Total annual pumpage at end of scenario:			10,000	25,000	40,000	50,000

[1]Annual pumped volumes of less than 5,000 acre-feet were constrained by a maximum drawdown of 1,000 feet in the pumping well.

Drawdown and discharge time series from 4 of 16 wells can be displayed simultaneously for the 200-year simulation period of a scenario (fig. 26; appendix F). All user-defined options are cells in the spreadsheet shown in figure 26 that are shaded gray. Drawdown or discharge is selected in row 27 and wells are selected in row 28. Discharges can be reported in units of cubic feet per day (CFD), acre-feet per year (ACRE-FT/YR), cubic feet per second (CFS), or gallons per minute (GPM) by selecting units in cell C25. Pumping scenarios: 10,000 acre-ft/yr, Limited (10K-L); 25,000 acre-ft/yr, Limited (25K-L); 50,000 acre-ft/yr, Limited (50K-L); and 50,000 acre-ft/yr, Unlimited (50K-U) are selected in cell E25. The same scenarios where 19,000 acre-ft/yr of irrigation also is simulated are identified as 10K-L+IRR, 25K-L+IRR, 50K-L+IRR, and 50K-U+IRR, respectively.

Simulated discharge reduction from selected control volumes and springs is the sum of all external sources and sinks in a control volume (appendix G, table 3). Discharge reduction from springs is the sum of well and drain packages in a flow-model cell, which is a control volume. Discharge reduction from 4 of 44 springs or control volumes can be displayed simultaneously for the 200-year simulation period

of a scenario (fig. 27; appendix G). All user-defined options are spreadsheet cells that are shaded gray. Springs or control volumes are selected in row 27 (fig. 27). Simulated discharge reductions can be reported in units of cubic feet per day (CFD), acre-feet per year (ACRE-FT/YR), cubic feet per second (CFS), or gallons per minute (GPM) by selecting units in cell C25. Pumping scenarios: 10,000 acre-ft/yr, Limited (10K-L); 25,000 acre-ft/yr, Limited (25K-L); 50,000 acre-ft/yr, Limited (50K-L); and 50,000 acre-ft/yr, Unlimited (50K-U) are selected in cell E25. The same scenarios where 19,000 acre-ft/yr of irrigation also is simulated are identified as 10K-L+IRR, 25K-L+IRR, 50K-L+IRR, and 50K-U+IRR, respectively.

Additional simulations can be tested by downloading the GBNP-C and GBNP-P models and selected supporting files (appendix H). All MODFLOW files and supporting utilities are in the zipped file, GBNP-USGS.zip. The supporting utilities are batch files, FORTRAN programs, and macros in Microsoft© Excel workbooks. The zip file contains subfolders for the geologic framework, FORTRAN programs, the calibration model (GBNP-C), the predictive model (GBNP-P) without existing irrigation, the predictive model (GBNP-P) with existing irrigation, and PostScript mapping instructions.
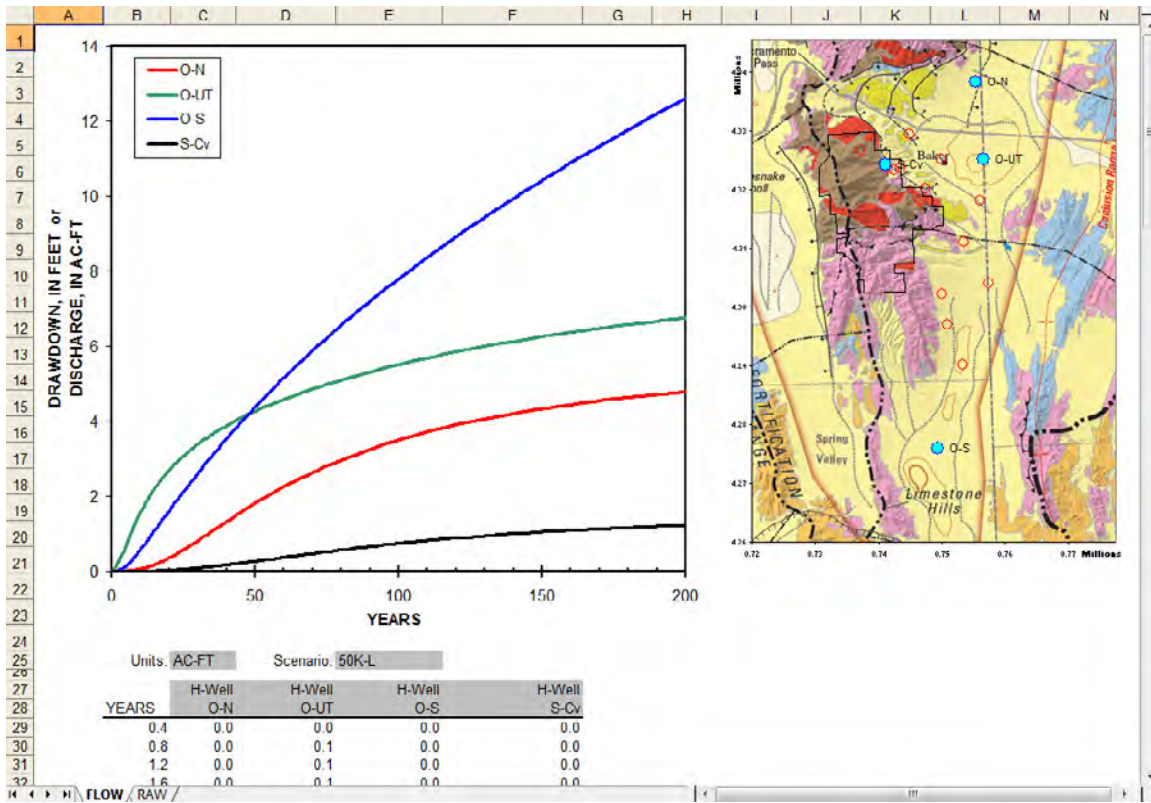
Figure 26. Example of drawdown and discharge time series from selected wells and observation points in Snake Valley east of Great Basin National Park.
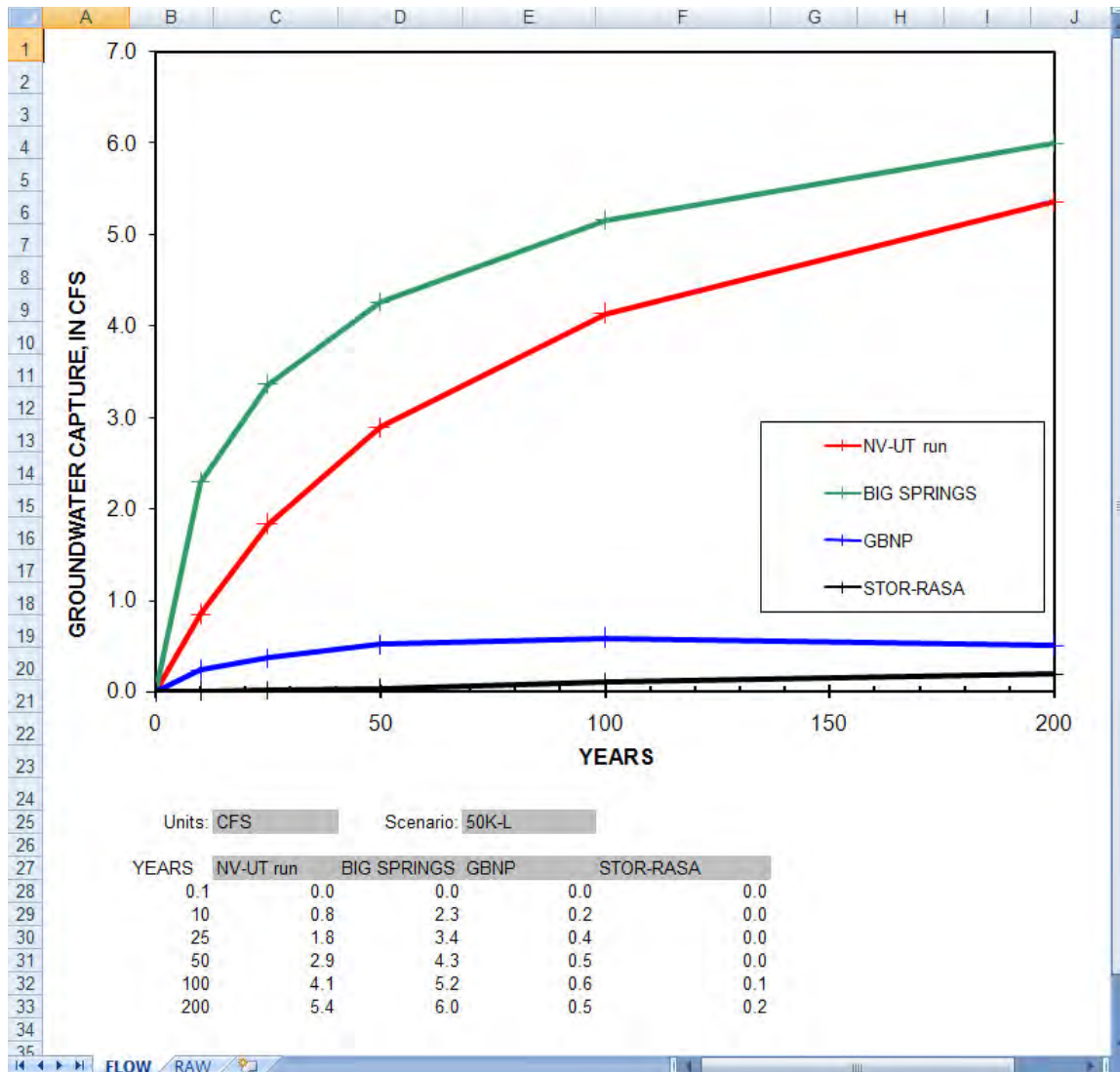
Figure 27. Example from appendix G of simulated reduction in spring discharges and capture from selected areas.

Model Limitations

The flow model addresses questions about regional groundwater flow and groundwater development in Spring and Snake Valleys, but cannot mimic exactly the actual system. This model, or any other model, is limited by simplification of the conceptual model, discretization effects, and difficulty in obtaining sufficient measurements to account for all spatial variation in hydraulic properties throughout the model area.

Measured groundwater levels and discharges were not matched perfectly by simulated observations, even after calibration, because errors cumulatively affect model results. These irreducible errors result from simplification of the conceptual model, grid scale, and insufficient measurements.

Lateral discretization of the study area into a rectangular grid of cells and vertical discretization into layers forced an averaging of hydraulic properties. Each cell represents a homogeneous block or some volumetric average of the aquifer medium. Discretization errors occurred in every model cell, which includes the smallest model cells. Bedding structures in the alluvium and fracture networks in the bedrock were averaged in these small cells that were 1,640 ft on a side and 10 ft thick. Flow paths are averaged over lengths of about 0.5 mi due to the averaging of the hydraulic properties.

The extent of drawdown predictions easily can be displaced 0.5 mi along the contact between basin fill and low permeability bedrock. These are areas where drawdown changes from less than 1 ft to more than 10 ft across distances of 0.5 mi or less (appendix E). A minimum uncertainty of 1,640 ft exists because of discretization errors. Projection of the mapped surface geology to the water table also contributed to uncertainty where the contact between basin fill and low permeability bedrock occurs in the saturated groundwater-flow system.

Errors in hydraulic diffusivity inversely affect the timing of groundwater capture. Hydraulic diffusivity is transmissivity divided by storage coefficient, which functionally is specific yield for unconfined aquifer conditions. Groundwater capture will occur sooner as hydraulic diffusivity increases and will be delayed as hydraulic diffusivity decreases. Errors in hydraulic-diffusivity estimates of 50 percent in the GBNP-P model are not unexpected so 50-percent errors in timing of groundwater-capture estimates can occur.

Drawdown and groundwater capture predictions will differ if recharge changes. Water levels will decline further than predicted if recharge decreases. For example, a 10 percent decrease in recharge would cause simulated water levels to decline 5 ft near Rowland Spring after 20 years. Water-level declines occur less quickly away from the recharge areas. Simulated water levels near Baker, Nevada, decline less than 5 ft, 200 years after decreasing recharge by 10 percent.

Transmissivity estimates likely are affected by compensating errors along the periphery of Spring and Snake Valleys. This is because these values contact the assigned hydraulic properties from the supporting RASA model outside of Spring and Snake Valleys. Compensating errors have a greater potential to affect results along the Confusion Range where transmissivity estimates exceed 10,000 ft²/d east of Snake Valley.

Summary

The National Park Service needs estimates of the potential effects of pumping from Snake Valley on springs, streams, and water levels in caves in and adjacent to Great Basin National Park. Understanding potential effects of pumping groundwater from Snake Valley is important because groundwater discharge to springs or streams in ecologically sensitive areas may be captured. The hydrologic effects of developing groundwater supplies are assessed using numerical, groundwater-flow models to estimate the timing and magnitude of capture from streams, springs, wetlands, phreatophytic plants, and water-table decline.

The study area was the 100,000 mi² carbonate-rock province of the Great Basin that was simulated previously for the Regional Aquifer-System Analysis, RASA Program of the Great Basin. The study area was much greater than Spring and Snake Valleys because pumping effects can propagate across multiple basins in the carbonate-rock province. Aquifers in the study area are basin fill and carbonate rock.

Spring and Snake Valleys are deep structural basins comprising carbonate and siliciclastic sedimentary rocks of Paleozoic age and igneous intrusive rocks of Jurassic to Tertiary age. Basin-fill deposits of Tertiary and Quaternary age and volcanic rocks of Tertiary age have accumulated in these structural basins, reaching thicknesses of more than 1 mile. Siliciclastic sedimentary rocks of Cambrian and older age and granitic rocks of Jurassic to Tertiary age are grouped together as a single hydrogeologic unit because both have low permeability. The thick sequences of basin-fill deposits and carbonate rocks can be very permeable and function as regional aquifers. Groundwater flow through basin fill occurs at depths shallower than 2,000 ft in Snake Valley because deeper sediments predominantly are clay and evaporite deposits as encountered in oil-well logs.

Transmissivity and specific yield of basin-fill and carbonate-rock aquifers were estimated from aquifer tests in Lake, Spring, and Snake Valleys. Transmissivity of the basin fill ranged from 1,200 to 12,000 ft²/d where basin-fill thickness exceeded 1,000 ft. Transmissivity of the carbonate rocks ranged from 10,000 to 55,000 ft²/d. Specific yield of the carbonate-rock and basin-fill aquifers averaged 2 and 15 percent, respectively.

The hydraulic conductivity of basin fill and transmissivity of basement-rock distributions in Spring and Snake Valleys were refined by calibrating a steady-state, three-dimensional, numerical groundwater-flow model of the carbonate-rock province to predevelopment conditions. Hydraulic properties and boundary conditions were defined primarily from the RASA model except in Spring and Snake Valleys. This locally refined model was referred to as the Great Basin National Park calibration or GBNP-C model. Groundwater flow through the study area was simulated with a 4-layer, finite-difference, MODFLOW model that extended from the water table to 2,000 ft below the water table in the basin fill.

Hydraulic conductivity and transmissivity were distributed throughout Spring and Snake Valleys with pilot points, which were mapped locations where hydraulic properties were assigned. Values at pilot points were interpolated to model cells with kriging in basin fill, basement rocks, and karst. Hydraulic conductivity of the basin fill was estimated because transmissivity is affected strongly by changes in saturated thickness near the edge of unconsolidated sediments. Transmissivity of the basement rocks was estimated because hydraulic conductivity is highly variable and thickness is correlated poorly with transmissivity. Continuity with the remainder of the RASA model area was maintained with additional pilot points that surrounded Spring and Snake Valleys.

Mountain-block and mountain-front recharges were distributed throughout Spring and Snake Valleys with pilot points and interpolated to model cells with kriging. Initial pilot-point values were sampled directly from the potential recharge distribution defined as annual precipitation in excess of 9.5 in.

Groundwater discharge from phreatophyte areas and springs was simulated as specified discharges in the GBNP-C model. Distributed groundwater-discharge estimates in Spring and Snake Valleys were specified directly from previous investigations. Spring discharges were specified at measured rates and sourced from model layers 2, 3, or 4. Groundwater discharge from the remainder of the GBNP-C model outside of Spring and Snake Valleys was simulated as specified in the original RASA model.

Recharge, hydraulic-conductivity, and transmissivity distributions of the GBNP-C model were estimated by minimizing a weighted composite, sum-of-squares objective function that included measurement and Tikhonov regularization observations. Measured water levels, simulated water levels from original RASA model, depth-to-water beneath distributed groundwater discharge and spring discharges, land-surface altitudes, spring discharge at Fish Springs, and changes in discharge on selected stream reaches were measurement observations. Tikhonov regularization observations were equations that defined preferred relations between the pilot points that defined recharge, hydraulic-conductivity, or transmissivity distributions. Ratios of initial recharge rates and homogeneity within simplified geologic classes were the preferred relations between pilot points. Regularization observations affected calibration most where the GBNP-C model was insensitive to measurement observations.

Simulated water levels compared favorably with target water levels and discharges for the model as a whole where the root mean square error for water levels was 39 ft. This error is small relative to the 5,400 ft range of measured water levels. Water-level residuals with absolute values greater than 50 ft were considered significant. Residuals were greatest where low permeability intrusive and volcanic rocks were simulated more accurately in Spring and Snake Valleys. Areas west of Spring Valley and surrounding southern Snake Valley were affected by a strong transmissivity contrast.

Transmissive structures were estimated consistently even though hydraulic property estimates at pilot points were non-unique. Areas of transmissivity in excess of 10,000 ft^2/d occurred along eastern Snake Valley and south of the Snake Range and persisted during all phases of model calibration. Simulated water levels were affected and flow was deflected from the east to the north by these structures.

The GBNP-C model simulated more groundwater flow through Spring and Snake Valleys than the original RASA model. This largely occurred because groundwater discharge from Spring and Snake Valleys in the GNBP-C model was 64,000 acre-ft/yr greater than in the RASA model. The GNBP-C model also simulated local flow in the mountain blocks that were not simulated by the RASA model. Simulated water budgets in the study area outside of Spring and Snake Valleys were similar in both the GNBP-C and RASA models.

The effects of uncertain distributed groundwater-discharge estimates in Spring and Snake Valleys on transmissivity estimates were bounded with alternative models. Specified annual distributed groundwater discharges from Spring and Snake Valleys simulated in the alternative models totaled 151,000 and 227,000 acre-ft. These were differences of 20 percent from the 187,000 acre-ft/yr specified in the calibrated GBNP-C model. Recharge changed about 10 percent more than changes in distributed groundwater discharge in the alternative models. Transmissivity estimates were minimally sensitive to groundwater-discharge estimates east of Great Basin National Park. Transmissivity estimates in the basin fill between Baker, Nevada, and Big Springs changed less than 50 percent between the two alternative models.

Potential effects of pumping from Snake Valley on springs, streams, and water levels in caves in and adjacent to Great Basin National Park were estimated with the Great Basin National Park predictive (GBNP-P) model. The GBNP-P model was a transient groundwater-flow model that simulated changes in groundwater storage. The hydraulic conductivity of basin fill and transmissivity of basement rock were the same distributions that were estimated with the GBNP-C model. Specific yields of 2 and 15 percent estimated from aquifer tests were specified for bedrock and basin fill, respectively, in the GBNP-P model based on surface geology. Groundwater capture and drawdown were simulated with a direct-drawdown approach in the GBNP-P model to reduce model complexity and uncertainty. Model input, other than the proposed pumpage, was limited to hydraulic-conductivity, transmissivity, specific yield, storage-coefficient, and groundwater-discharge distributions.

Capture of distributed groundwater and spring discharge were simulated in the GBNP-P model using a combination well and drain packages in MODFLOW. Maximum simulated groundwater capture was constrained by the mapped or measured distributed groundwater or spring discharge rates. Capture of discharge to streams in low permeability mountain blocks was simulated with specified heads set to zero.

Hydraulic property distributions from the alternative models were not considered because the range of pumping rates investigated was greater than transmissivity differences between alternative models. Specific yield was the significant component of groundwater storage in the GBNP-P model. Reasonable hydraulic-diffusivity estimates in Snake Valley south of U.S. Highway 50 could deviate from the assigned values in the GBNP-P model by as much as 50 percent.

Four groundwater-development scenarios were investigated where total annual withdrawals ranged from 10,000 to 50,000 acre-ft during a 200-year pumping period. Four additional scenarios also were simulated that added the effects of existing pumpage in Snake Valley. Potential groundwater withdrawal locations were limited to nine proposed points of diversion. Pumpage from the proposed points of diversion was distributed between 60 ft and 2,060 ft below the water table and the maximum drawdown was limited to 1,000 ft in three of four scenarios. Results from the GBNP-P model scenarios are presented as maps of groundwater capture and drawdown, time series of drawdowns and discharges from selected wells, and time series of discharge reductions from selected springs and control volumes.

Simulated drawdown propagation was attenuated where groundwater discharge could be captured. General patterns of groundwater capture and water-table declines were similar for all scenarios. Simulated drawdowns greater than 1 ft propagated outside of Spring and Snake Valleys after 200 years of pumping in all scenarios.

References Cited

Belcher, W.R., ed., 2004, Death Valley regional ground-water flow system, Nevada and California—Hydrogeologic framework and transient ground-water flow model: U.S. Geological Survey Scientific Investigations Report 2004-5205, 408 p. (Also available at http://pubs.usgs.gov/sir/2004/5205/.)

Belcher, W.R., Elliott, P.E., and Geldon, A.L., 2001, Hydraulic-property estimates for use with a transient ground-water flow model of the Death Valley regional ground-water flow system, Nevada and California: U.S. Geological Survey Water-Resources Investigations Report 01-4210, 28 p. (Also available at http://pubs.usgs.gov/wri/wri014210/.)

Blankennagel, R.K., and Weir, J.E., Jr., 1973, Geohydrology of the eastern part of Pahute Mesa, Nevada Test Site, Nye County, Nevada: U.S. Geological Survey Professional Paper 712-B, 35 p.

Bredehoeft, J., and Durbin, T., 2009, Ground water development—The time to full capture problem: Ground Water, v. 47, issue 4, p. 506–514.

Bunch, R.L., and Harrill, J.R., 1984, Compilation of selected hydrologic data from the MX missile-siting investigation, east-central Nevada and western Utah: U.S. Geological Survey Open-File Report 84-702, 123 p.

Daly, Christopher, Neilson, R.P., and Phillips, D.L., 1994, A statistical-topographic model for mapping climatological precipitation over mountainous terrain: Journal of Applied Meteorology, v. 33, no. 2, p. 140–158, accessed December 17, 2010, at http://alpha.es.umb.edu/~david.tenenbaum/eeos465/daly.pdf.

Doherty, John, 2003, Ground water model calibration using pilot points and regularization: Ground Water, v. 41, issue 2, p. 170–177. doi:10.1111/j.1745-6584.2003.tb02580.x, accessed December 17, 2010, at http://onlinelibrary.wiley.com/doi/10.1111/j.1745-6584.2003.tb02580.x/abstract.

Doherty, John, 2008a, PEST: Model-independent parameter estimation, user manual, 5th ed.: Brisbane, Australia, Watermark Numerical Computing, accessed April 1, 2009, http://www.pesthomepage.org/Downloads.php#hdr1.

Doherty, John, 2008b, PEST Groundwater data utilities: Brisbane, Australia, Watermark Numerical Computing, accessed April 1, 2009, http://www.pesthomepage.org/Downloads.php#hdr1.

Doherty, John, and Johnston, J.M., 2003, Methodologies for calibration and predictive analysis of a watershed model: Journal of the American Water Resources Association, v. 39, no. 2, p. 251–265.

Durbin, Timothy, Delemos, David, and Rajagopal-Durbin, Aparna, 2008, Application of superposition with nonlinear head-dependent fluxes: Ground Water, v. 46, issue 2, p. 251–258, doi:10.1111/j.1745-6584.2007.00408.x, accessed December 17, 2010, at http://onlinelibrary.wiley.com/doi/10.1111/j.1745-6584.2007.00408.x/full.

Elliott, P.E., Beck, D.A., and Prudic, D.E., 2006, Characterization of surface-water resources in the Great Basin National Park area and their susceptibility to ground-water withdrawals in adjacent valleys, White Pine County, Nevada: U.S. Geological Survey Scientific Investigations Report 2006-5099, 156 p. (Also available at http://pubs.usgs.gov/sir/2006/5099/.)

Ertec Western, Inc., 1981, MX Siting Investigation, Water Resources Program, Technical Summary Report, Volume I: Long Beach, Calif.: Long Beach, CA, prepared for the Department of the Air Force, Ballistic Missile Office, Report E-TR-52-I, 97 p.

Faunt, C.C., Blainey, J.B., Hill, M.C., D'Agnese, F.A., and O'Brien, G.M., 2004, Transient flow model, in Belcher, W.R., ed., Death Valley regional ground-water flow system, Nevada and California—Hydrogeologic framework and transient ground-water flow model: U.S. Geological Survey Scientific-Investigations Report 2004-5205, p. 257–352. (Also available at http://pubs.usgs.gov/sir/2004/5205/pdf/Chapter_F.pdf.)

Fienen, M.N., Muffels, C.T., and Hunt, R.J., 2009, On constraining pilot point calibration with regularization in PEST: Ground Water, v. 47, issue 6, p. 835–844, doi:10.1111/j.1745-6584.2009.00579.x, accessed December 17, 2010, at http://onlinelibrary.wiley.com/doi/10.1111/j.1745-6584.2009.00579.x/full.

Flint, A.L., and Flint, L.E., 2007, Application of the basin characterization model to estimate in-place recharge and runoff potential in the Basin and Range carbonate-rock aquifer system, White Pine County, Nevada, and adjacent areas in Nevada and Utah: U.S. Geological Survey Scientific Investigations Report 2007-5099, 20 p. (Also available at http://pubs.usgs.gov/sir/2007/5099/.)

Freeze, R.A., and Witherspoon, P.A., 1967, Theoretical analysis of regional ground-water flow: 2. Effect of water-table configuration and subsurface permeability variation: Water Resources Research, v. 3, no. 2, p. 623–634.

Glover, R.E., and Balmer, G.G., 1954, River depletion resulting from pumping a well near a river: Transactions of the American Geophysical Union, v. 35, p. 468–470.

Halford, K.J., 2006, MODOPTIM: A general optimization program for ground-water flow model calibration and ground-water management with MODFLOW: U.S. Geological Survey Scientific Investigation Report 2006-5009, 62 p. (Also available at http://pubs.usgs.gov/sir/2006/5009/.)

Halford, K.J., and Hanson, R.T., 2002, User guide for the drawdown-limited, Multi-Node Well (MNW) Package for the U.S. Geological Survey's modular three-dimensional finite-difference ground-water flow model, versions MODFLOW–96 and MODFLOW–2000: U.S. Geological Survey Open-File Report 02–293, 33 p. (Also available at http://pubs.usgs.gov/of/2002/ofr02293/text.html.)

Harbaugh, A.W., Banta, E.R., Hill, M.C., and McDonald, M.G., 2000, MODFLOW-2000, the U.S. Geological Survey modular ground-water model—User guide to modularization concepts and the ground-water flow process: U.S. Geological Survey Open-File Report 00-92, 121 p. (Also available at http://water.usgs.gov/nrp/gwsoftware/modflow2000/ofr00-92.pdf.)

Hardman, George, 1936, Nevada precipitation and acreages of land by rainfall zones: Reno, University of Nevada Agricultural Experiments Station report, 10 p. and map.

Harrill, J.R., Gates, J.S., and Thomas, J.M., 1988, Major ground-water flow systems in the Great Basin region of Nevada, Utah, and adjacent States: U.S. Geological Survey Hydrologic Investigations Atlas HA-694-C, scale 1:1,000,000, 2 sheets.

Harrill, J.R., and Prudic, D.E., 1998, Aquifer systems in the Great Basin region of Nevada, Utah, and adjacent States— Summary report: U.S. Geological Survey Professional Paper 1409-A, 66 p.

Hose, R.K., Blake, M.C., Jr., and Smith, R.M., 1976, Geology and mineral resources of White Pine County, Nevada: Nevada Bureau of Mines and Geology Bulletin 85, 105 p.

Isaaks, E.H., and Srivastava, R.H., 1989, An Introduction to Applied Geostatistics: New York, Oxford University Press, 561 p.

Leake, S.A., Greer, William, Watt, Dennis, and Weghorst, Paul, 2008, Use of superposition models to simulate possible depletion of Colorado River water by ground-water withdrawal: U.S. Geological Survey Scientific Investigations Report 2008-5189, 25 p. (Also available at http://pubs.usgs.gov/sir/2008/5189/.)

Leake, S.A., Reeves, H.W., and Dickinson, J.E., 2010, A New Capture Fraction Method to Map How Pumpage Affects Surface Water Flow. Ground Water, 48: 690–700. doi: 10.1111/j.1745-6584.2010.00701.x

Leeds, Hill and Jewett, Inc., 1981, Groundwater investigation – Phase 2 – Technical report for the White Pine Power Project: San Francisco, CA, prepared for Los Angeles Department of Water and Power.

Leeds, Hill and Jewett, Inc., 1983, Groundwater Investigation – Phase 3 – Technical report for the White Pine Power Project: San Francisco, CA, prepared for Los Angeles Department of Water and Power.

Maxey, G.B., and Eakin, T.E., 1949, Ground water in White River Valley, White Pine, Nye, and Lincoln Counties, Nevada: Nevada State Engineer, Water Resources Bulletin 8, 59 p.

McDonald, M.G., and Harbaugh, A.W., 1988, A modular three-dimensional finite-difference ground-water flow model: U.S. Geological Survey Techniques of Water-Resources Investigations, book 6, chap. A1, 586 p. (Also available at http://pubs.usgs.gov/twri/twri6a1/.)

Moreo, M.T., Halford, K.J, LaCamera, R.J., and Laczniak, R.J., 2003, Estimated ground-water withdrawals from the Death Valley Regional Flow System, Nevada and California, 1913–98: U.S. Geological Survey Water-Resources Investigations Report 03-4245, 28 p.

Moreo, M.T., Laczniak, R.J., and Stannard, D.I., 2007, Evapotranspiration rate measurements of vegetation typical of ground-water discharge areas in the Basin and Range carbonate-rock aquifer system, White Pine County, Nevada, and adjacent areas in Nevada and Utah, September 2005–August 2006: U.S. Geological Survey Scientific Investigations Report 2007-5078, 36 p. (Also available at http://pubs.usgs.gov/sir/2007/5078/.)

National Park Service, 2007, Digital geologic map of Great Basin National Park and vicinity, Nevada: National Park Service Geologic Resource Evaluation (GRE) program, digital GIS data and ancillary tables, scale 1:24,000, accessed December 17, 2010, at http://science.nature.nps.gov/nrdata/datastore.cfm?ID=44849.

Nevada Bureau of Mines and Geology, 2008, Oil and gas by API number: accessed December 17, 2010, at http://www.nbmg.unr.edu/lists/oil/logs/Oil_and_Gas_by_API.htm.

Nevada Division of Water Resources, 2008, Snake Valley water right applications: State Engineer's Interim Order no. 2, October 28, 2008, accessed December 17, 2010, at http://water.nv.gov/Hearings/waterhearing/snakevalley/documents/Int%20order%202.pdf.

PRISM Group, 2006, United States average monthly or annual precipitation, 1971–2000: Corvallis, OR, PRISM Group at Oregon State University, accessed December 18, 2010, at http://www.prism.oregonstate.edu.

Prudic, D.E., Harrill, J.R., and Burbey, T.J., 1995, Conceptual evaluation of regional ground-water flow in the carbonate-rock province of the Great Basin, Nevada, Utah, and adjacent States: U.S. Geological Survey Professional Paper 1409-D, 102 p.

RamaRao, B.S., LaVenue, A.M., De Marsily, Ghislain, and Marietta, M.G., 1995, Pilot point methodology for automated calibration of an ensemble of conditionally simulated transmissivity fields: 1. Theory and computational experiments: Water Resources Research, v. 31, no. 3, p. 475–493.

Reheis, Marith, 1999, Extent of Pleistocene lakes in the western Great Basin: U.S. Geological Survey Miscellaneous Field Studies Map MF-2323, scale 1:800,000. (Also available at pubs.usgs.gov/mf/1999/mf-2323/.)

Rush, F.E., 1974, Static ground water levels of Nevada: Nevada Department of Conservation and Natural Resources, Division of Water Resources map, 1 sheet, scale 1:750,000.

Schaefer, D.H., and Harrill, J.R., 1995, Simulated effects of proposed ground-water pumping in 17 basins of east-central and southern Nevada: U.S. Geological Survey Water-Resources Investigations Report 95-4173, 71 p.

Smith, J.L., Laczniak, R.J., Moreo, M.T., and Welborn, T.L., 2007, Mapping evapotranspiration units in the Basin and Range carbonate-rock aquifer system, White Pine County, Nevada, and adjacent areas in Nevada and Utah: U.S. Geological Survey Scientific Investigations Report 2007-5087, 20 p. (Also available at http://pubs.usgs.gov/sir/2007/5087/.)

Southern Nevada Water Authority, 2009, Transient numerical model of groundwater flow for the Central Carbonate-Rock Province—Clark, Lincoln, and White Pine Counties Groundwater Development Project. Prepared in cooperation with the Bureau of Land Management: Southern Nevada Water Authority, Las Vegas, Nevada, 394 p.

Stratigraphic Committee of the Eastern Nevada Geological Society (Langenheim, R.L., Jr., and Larson, E.R., Cochairmen), 1973, Correlation of Great Basin Stratigraphic Units: Nevada Bureau of Mines and Geology Bulletin 72, 36 p., 3 charts.

Sweetkind, D.S., Knochenmus, L.A., Ponce, D.A., Wallace, A.R., Scheirer, D.S., Watt, J.T., and Plume, R.W., 2007, Hydrogeologic framework, in Welch, A.H., Bright, D.J., and Knochenmus, L.A., eds., Water resources of the Basin and Range carbonate-rock aquifer system, White Pine County, Nevada and adjacent areas in Nevada and Utah: U.S. Geological Survey Scientific Investigations Report 2007-5261, p. 11–36. (Also available at http://pubs.usgs.gov/sir/2007/5261/.)

Theis, C.V., 1935, The relation between the lowering of the piezometric surface and the rate and duration of discharge of a well using ground-water storage: Transactions of the American Geophysical Union, v. 16, p. 519–524.

Tóth, József, 1962, A theory of groundwater motion in small drainage basins in central Alberta, Canada: Journal of Geophysical Research, v. 67, no. 11, p. 4375–4387.

U.S. Geological Survey, 1999, National Elevation Dataset (NED): Sioux Falls, SD, U.S. Geological Survey, EROS Data Center, accessed December 17, 2010, at http://seamless.usgs.gov.

U.S. Geological Survey, 2010, Aquifer tests: Carson City, Nevada, U.S. Geological Survey, Nevada Water Science Center, accessed February 14, 2010, at http://nevada.usgs.gov/water/aquifertests/index.htm.

Watt, J.T., and Ponce, D.A., 2007, Geophysical framework investigations influencing ground-water resources in east-central Nevada and west-central Utah, with a section on Geologic and geophysical basin-by-basin descriptions by Wallace, A.R., Watt, J.T., and Ponce, D.A.: U.S. Geological Survey Open-File Report 2007-1163, 43 p., 2 pls., scale 1:750,000.

Welborn, T.L., and Moreo, M.T., 2007, Irrigated acreage within the Basin and Range carbonate-rock aquifer system, White Pine County, Nevada, and adjacent areas in Nevada and Utah: U.S. Geological Survey Data Series 273, 18 p. (Also available at http://pubs.usgs.gov/ds/2007/273/.)

Welch, A.H., Bright, D.J., and Knochenmus, L.A., 2007, Water resources of the Basin and Range carbonate-rock aquifer system, White Pine County, Nevada, and adjacent areas in Nevada and Utah: U.S. Geological Survey Scientific Investigations Report 2007-5261, 96 p. (Also available at http://pubs.usgs.gov/sir/2007/5261/.)

Western Regional Climate Center, 2009, Nevada and Utah climate summaries 1971 to 2000: accessed December 17, 2010, http://www.wrcc.dri.edu/summary/Climsmut.html.

Wilson, J.W., 2007, Water-level surface maps of the carbonate-rock and basin-fill aquifers in the Basin and Range carbonate-rock aquifer system, White Pine County, Nevada, and adjacent areas in Nevada and Utah: U.S. Geological Survey Scientific Investigations Report 2007-5089, 10 p. (Also available at http://pubs.usgs.gov/sir/2007/5089/.)

Winograd, I.J., and Thordarson, W., 1975, Hydrogeologic and hydrochemical framework, south-central Great Basin, Nevada-California, with special reference to the Nevada Test Site: U.S. Geological Survey Professional Paper 712-C, 125 p.

Zaadnoordijk, W.J., 2009, Simulating piecewise-linear surface water and ground water interactions with MODFLOW: Ground Water, v. 47, issue 5, p. 723–726, doi:10.1111/j.1745-6584.2009.00582.x, accessed December 17, 2010, at http://onlinelibrary.wiley.com/doi/10.1111/j.1745-6584.2009.00582.x/full.

This page intentionally left blank.

Appendix A. Water-Level Observations

Observation wells, easting, northing, measured water levels, site identifier, local names, and identifier for PEST (Doherty, 2008a) are tabulated in a Microsoft© Excel workbook and can be accessed and downloaded at http://pubs.usgs.gov/sir/2011/5032/.

Appendix B. Results from GBNP-C Model

Maps of calibrated recharge, hydraulic conductivity, and transmissivity distributions with pilot points and estimated values posted. Maps of calibrated, predevelopment water levels with measured water levels and residuals posted. These maps are available in PDF format and can be accessed and downloaded at http://pubs.usgs.gov/sir/2011/5032/.

Appendix C. Residuals from GBNP-C Model

Residuals from water levels, evapotranspiration, land-surface altitude, and springs representative of predevelopment groundwater conditions are tabulated and can be displayed interactively from a Microsoft© Excel workbook and can be accessed and downloaded at http://pubs.usgs.gov/sir/2011/5032/. The workbook is designed to view residuals by threshold values, layer, and observation type.

Appendix D. Pilot-Point Values for all Models

Pilot point name for PEST (Doherty, 2008a), easting, northing, model layer, thickness of cell with pilot point, type, lithology of cell for the GBNP-C, GBNP-LowET, and GBNP-HighET models are tabulated in a Microsoft© Excel workbook and can be accessed and downloaded at http://pubs.usgs.gov/sir/2011/5032/. Pilot points are grouped by recharge, hydraulic conductivity, and transmissivity.

Appendix E. Predicted Drawdown Maps

Maps of drawdown and captured groundwater discharge from the four proposed development scenarios of pumping 10,000; 25,000; 40,000; and 50,000 acre-ft/yr. Maps are presented by model layer at 10, 25, 50, 100, and 200 years after pumping began for the four proposed development scenarios. These maps are available in PDF format and can be accessed and downloaded at http://pubs.usgs.gov/sir/2011/5032/.

Appendix F. Predicted Time Series from Wells

Time series of drawdowns and discharges from selected wells are tabulated and can be displayed interactively from a Microsoft© Excel workbook and can be accessed and downloaded at http://pubs.usgs.gov/sir/2011/5032/. The workbook is designed to simultaneously view as many as four time series.

Appendix G. Predicted Time Series from Springs

Time series of discharge reductions from selected springs and control volumes are tabulated and can be displayed interactively from a Microsoft© Excel workbook and can be accessed and downloaded at http://pubs.usgs.gov/sir/2011/5032/. The workbook is designed to simultaneously view as many as four time series.

Appendix H. MODFLOW Files and Supporting Utilities

All MODFLOW files and supporting utilities are in the zipped file, sir20115032_appH.zip can be accessed and downloaded at http://pubs.usgs.gov/sir/2011/5032/. The supporting utilities are batch files, FORTRAN programs, and macros in Microsoft© Excel workbooks. The zip file contains subfolders for the geologic framework, FORTRAN programs, the calibration model (GBNP-C), the predictive model (GBNP-P) without existing irrigation, the predictive model (GBNP-P) with existing irrigation, and PostScript mapping instructions. Contents of all subdirectories and necessary software are reported in README file in the root directory of the unzipped GBNP-USGS.zip file.